
Zewail City for Science and Technology

University of Science and Technology

**Renewable Energy Engineering Program**

# Development of Lithium-Ion Battery Management System for Electric Vehicles

A Graduation Project submitted in Partial Fulfillment of B.Sc. Degree Requirements in Renewable Energy Engineering.

**Prepared By:**

Mohamed Ali Moustafa 201800271

Bavly Atef Abdelnour 201800869

Mohamed Khalid Mohamed 201800054

Mahmoud Abdelhaalim 201800492

**Supervised By:**

Dr. Amgad Amin Eldeib

**2022/2023**

## Acknowledgment

This work is under the supervision of Dr. Amgad Eldeib who has always been supportive and helping in developing the idea from scratch till it’s been a complete system of its own.

Dr. Mohamed Lotfi Eid Shaltout has always been keen and available for help and guiding through the development phase and creating suitable scope for the project.

# Contents

# Table of figures and tables.

# Table of Equations.

# 1 Abstract

The battery is the most crucial, costly, and controversial component of an electric car. Critics of electric vehicles often point to the battery as the primary issue, citing high costs, limited lifespan, and the need for early replacement, limited range, and negative impact on the environment when disposing of them. While some of these concerns were once valid, they are no longer relevant today. This article will examine all of these topics, starting with the design of batteries, their key specifications, and focusing in-depth on their capacity, range, lifespan, and proper maintenance. Additionally, it will explore what happens to the battery after 15 years of use when it can no longer fulfill its original purpose. Lastly, for those interested, there will be a brief overview of the evolution of batteries for electric vehicles.

## 1.1 Expected outcomes

- A fully defined Lithium-ion battery model.
- Baselines for the approaches of SOC estimation, SOH estimation, cell balancing, and battery charging and discharging control.

# 2 Simulink Blocks

- Goto
- From
- Constant
- Add
- Not
- Gain
- Ideal Switch
- Switch
- Mosfet
- Voltage source
- Battery
- Bus selector
- Diode
- Series RLC Branch
- Display
- Scope
- To Workspace
- Power GUI
- PWM generator
- PI Controller
- MATLAB Function
- Rate Transition
- Array
- Selector
- Vector Concentrator
- Unit Delay

# 3 Nomenclature and list of abbreviations

BMS: Battery Management System

SOC: State of Charge

SOH: State of Health

EV: Electric Vehicle

CCCV: Constant Current Constant Voltage

# 4 Introduction

## 4.1 Problem Statement

The Promising technology of electric vehicles has created enforced the batteries industry into developing a more save, efficient, and affordable technology to adapt with the market requirements. The most important aspect in any developing technology is related to the safety of the system and portability and maintainability. Lithium-ion batteries have a high energy density and can build high voltage configurations which make the battery system need a high protection level to protect the system from any electrical failures or high voltage / high current issues. The thermal issues of high current flow and non-balanced state of charge of each cell among the system could lead to any thermal issues, therefore, reducing the life-time of the battery. The main statement of this project is to provide a handy solution for SOC estimation, SOH estimation, power balancing, charging and discharging control to monitor the performance of the battery.

## 4.2 Battery Design

The batteries used in electric cars vary from one manufacturer to another, with each company producing slightly different batteries that function through different chemical reactions. Despite these differences, the basic construction of the batteries remains the same, made up of basic battery cells and modules.

Batteries consist of hundreds, or even thousands, of small battery cells connected in either a series or parallel connection to provide the required voltage and current. Each battery cell has a voltage of 3-4V, and there are currently three types used: cylindrical, prismatic, and pouch. Tesla uses cylindrical cells, which are mature, cost-effective, and highly efficient. BMW and Volkswagen use prismatic cells, which are more compact and easier to cool, but have a lower energy density and issues with the number of charge and discharge cycles. Nissan, Renault, and Chevrolet use pouch batteries, which offer the most flexible design and capacity, but require careful control of temperature and pressure.

The battery cells form battery modules, which serve as the building blocks for each battery. This arrangement makes production, installation, management, and maintenance easier, and individual modules can be replaced if necessary. Additionally, in the event of a fire, the modules can help reduce the rate of its spread.

The battery modules include a cooling unit, a temperature monitor, and a voltage monitor, which send information to the Battery Management System (BMS). The BMS then manages the optimal environment for the battery. The modules also have relays and other components to ensure proper electricity and voltage distribution. As a result, it is possible to ensure that all cells are charged and discharged evenly, which greatly impacts the battery life of the electric car. The batteries used in electric cars vary from one manufacturer to another, with each company producing slightly different batteries that function through different chemical reactions. Despite these differences, the basic construction of the batteries remains the same, made up of basic battery cells and modules.

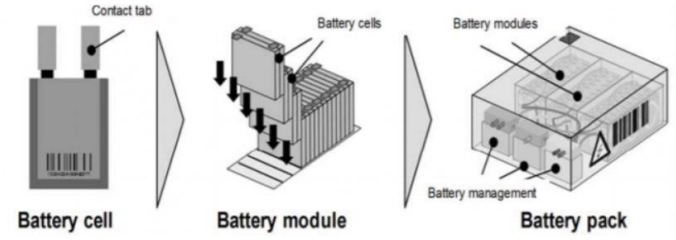


*Figure 4-1 Battery construction levels*

### 4.2.1 Important Battery Parameters

The design and production of batteries for electric vehicles must meet a number of important criteria. The weight and size of the battery are crucial due to the mobility of the car, which is why researchers and manufacturers focus on energy density, or the amount of energy per unit of weight or volume. There is ongoing competition to produce batteries with the highest possible energy density, some focusing on the energy density of individual cells, while others focus more on the density of the entire module, taking into account the shape of the battery cells and their arrangement.

Another important factor is the number of charge and discharge cycles the battery can endure without losing its properties, which reflects the overall battery life. Most batteries last between 1000 to 1500 cycles, but some have already been developed to withstand up to 7000 charges. Cost is also a key consideration, accounting for about 30% of the total price of an electric car. Typically, the cost is expressed as the price per unit of energy, usually in USD per kWh. In 2010, the cost was 1100 USD/kWh, but by 2019 it had dropped to 156 USD/kWh, and it is expected to fall further to 100 USD/kWh by 2024, due to improved battery efficiency, higher energy density, and more efficient production processes. The reduction in battery cost is expected to bring the cost of electric vehicles more in line with traditional gas-powered cars.

### 4.2.2 Battery Operation Area

Electric car batteries are not just a single unit, but are actually composed of many smaller battery cells that are combined into modules and then put together to form a battery pack. This arrangement makes it easier to manufacture, install, and maintain the battery, while also allowing for the necessary capacity and energy. The batteries used in electric cars are typically lithium-based, which is currently the most efficient technology available. However, lithium batteries can be affected by temperature changes, overcharging or discharging, and temperature leaks, so it's important to carefully monitor these conditions to ensure the battery's longevity. To maximize battery performance, it's crucial to maintain the battery within the "Safety Operation Area," which includes a temperature range of -5 to 45°C, a voltage range of 2 to 4 volts, and a current range of 0 to 1A.

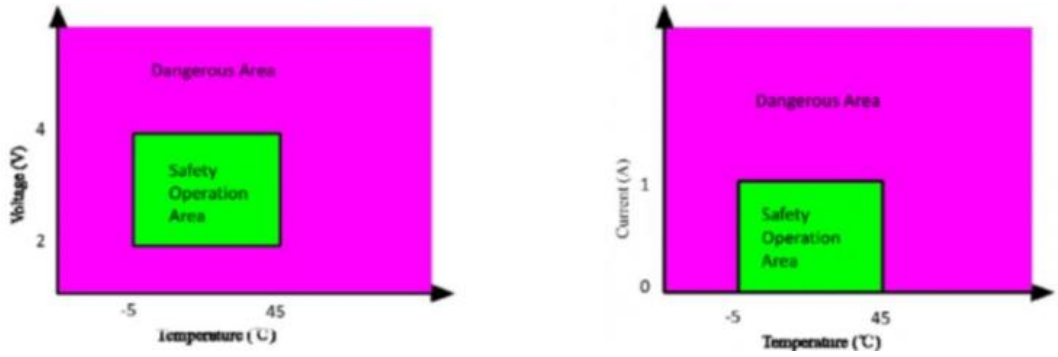


*Figure 4-2 Effect of Temperature on operational region*

## 4.3 Battery Capacity and Range

The range and capacity of an electric car battery, which are crucial factors, are determined by several key features. Efforts are made to balance weight, price, and range based on the current technology. The capacities of the batteries currently available on the market range from 16 kWh (Mitsubishi and MiEV) to 90 kWh (Tesla S). On average, lead batteries have a range of 30-80 km, nickel batteries can reach up to 200 km, and lithium batteries can go 320-480 km. The use of regenerative braking, which recycles energy from braking to be used again, can increase the range by 10-15% in regular city traffic and up to 50% in extreme conditions. The range of the battery is also influenced by weather, with the use of heating or air conditioning reducing the range in extreme conditions by up to 96 km. Other factors such as terrain, driving skills, weight, and type of vehicle also affect the battery's range, just like in traditional internal combustion engines.

## 4.4 Battery Lifespan

A common worry among electric car owners is the potential for an early loss in battery capacity and the need for a replacement. However, this fear is often unfounded, as most drivers have found that the advanced battery management systems (BMS) in modern electric cars prevent this from happening.

The battery is charged by the on-board charger and charging stations, which communicate with each other to ensure that charging does not negatively impact the battery's lifespan. For example, the Nissan LEAF electric car, which sold over 250,000 units between 2010 and 2016, only had to replace 0.01% of its batteries due to internal defects. Most vehicles were driven over 200,000 kilometers while retaining 90% of their battery capacity. Tesla Roadsters have also maintained 80-85% of their battery capacity even after 160,000 kilometers, regardless of the climate in which they were used.

In cases where some cells in the battery do become defective, they can easily be replaced due to the modular design of the battery, and the car can continue to operate normally. Tesla Model S batteries come with an 8-year warranty, and lithium batteries paired with solar panels are estimated to have a lifespan of over 20 years.

### 4.4.1 Battery Care, Second Life, and Recycling

Battery longevity and performance depend not only on the type of battery and the chemical reaction that occurs within it, but also on the driver's behavior and maintenance. Deep-cycle lithium batteries should never be depleted below 20% of their total capacity. Some newer models can be depleted a bit more, but never to the point of complete discharge.

To prevent excessive depletion, some manufacturers limit a portion of the battery's capacity. For instance, Ford now indicates the usable battery capacity in its vehicles. It is also important to charge the battery using slow AC charging stations when possible. High-power DC charging stations, over 20 kW, are designed for long-distance travel and should not be overused.

When a battery is no longer suitable for use in an electric vehicle, there are two options: second-life use or recycling. The former involves giving the battery a new purpose as stationary energy storage. Batteries can help solve the issue of discrepancy between renewable energy production and consumption by providing storage options. The final option, recycling, involves recovering as much of the used material as possible with minimal energy expenditure. European directives require manufacturers to collect and recycle batteries at their own cost. The most challenging part of recycling is directly processing the battery cells and separating the metals used in the chemical reactions, although up to 85% efficiency can still be achieved with cobalt.

## 4.5 Batteries Development and Their Future

The history of electric vehicle (EV) batteries dates back to the beginning of the 20th century, when the first electric cars utilized lead batteries. Lead batteries were accessible and cost-effective, but they had a few drawbacks like they shouldn't be discharged below 50% and required regular electrolyte monitoring. They were also quite heavy, accounting for 25-50% of the electric car's weight, and had a lifespan of about three years. Lead batteries had low specific energy, around 30-50 Wh/kg, with an efficiency of 70-75%, and reduced performance in cold weather.

Later, nickel-metal hydride batteries emerged as an improvement over lead batteries with a better specific energy and longer service life. For example, the battery in the first Toyota RAV4

hybrid car is still functional after more than 10 years and 160,000 kilometers. However, these batteries had low efficiency, high self-discharge rates, and poor performance in cold weather.

The invention of Zebra batteries helped overcome some of these challenges, but they had their own limitations like needing initial heating to reach 270°C, low power, and a risk of discharge. The lithium-ion battery was first introduced in 1979 and remains one of the most commonly used batteries. The early prototypes had some problems with temperature sensitivity, deformation at high temperatures, low performance in low temperatures, and early degradation.

The current generation of lithium-ion batteries offers longer life, environmental protection, reduced risk of fire, and faster charging speed at the cost of some specific energy and power. Lithium-phosphate batteries last more than 10 years and can be charged more than 7,000 times. Researchers are exploring two main options for the future of EV batteries: preserving lithium batteries but replacing graphite with silicon to increase specific energy and energy density, or solid batteries that don't use electrolytes for even greater safety and lifespan. Commercial production of solid batteries is estimated to be available in 10 years.

## 4.6 Environmental Impact of Lithium-ion Batteries

1. Extraction of raw materials: The mining and extraction of lithium, cobalt, nickel, and other metals required for battery production can have negative environmental impacts. It can lead to habitat destruction, deforestation, soil erosion, and water pollution. Additionally, some mining practices may involve the use of toxic chemicals that can harm ecosystems and human health.

2. Greenhouse gas emissions: The manufacturing process of lithium-ion batteries involves significant energy consumption and can contribute to greenhouse gas emissions. This includes the extraction and processing of raw materials, the manufacturing of battery components, and the assembly of the battery cells.

3. Water consumption: The production of lithium-ion batteries requires substantial amounts of water for mining, refining, and processing raw materials. In regions already facing water scarcity, increased demand for water in battery production can strain local water resources.

4. Battery disposal: The disposal of lithium-ion batteries poses environmental challenges. If not properly managed, they can release toxic chemicals and heavy metals into the environment, leading to soil and water contamination. The improper disposal or incineration of lithium-ion batteries can also contribute to air pollution.

5. Resource depletion: Lithium, cobalt, and nickel are finite resources, and the increasing demand for these metals in battery production raises concerns about resource depletion. Additionally, the extraction of these resources can have social and environmental implications in regions where mining takes place.

## 4.7 Standards and Regulations of Lithium-ion Batteries

Lithium-ion batteries are subject to various standards and regulations to ensure their safety, performance, and compatibility. Here are some of the key standards that govern lithium-ion batteries:

1. IEC 62133: This is an international safety standard developed by the International Electrotechnical Commission (IEC) specifically for lithium-ion batteries used in portable devices. It includes requirements for the design, construction, and testing of batteries to ensure their safe operation.

2. UN 38.3: This standard is established by the United Nations (UN) and is specific to the transportation of lithium-ion batteries. It sets out the requirements for packaging, testing, and labeling of batteries to ensure their safe transport by air, sea, or road.

3. UL 1642 and UL 2054: These are safety standards developed by Underwriters Laboratories (UL) for lithium-ion batteries used in various applications. UL 1642 focuses on the safety of individual cells or batteries, while UL 2054 covers the safety requirements for complete battery systems used in portable devices.

4. ISO 12405: This standard provides guidelines for the testing and characterization of lithium-ion batteries for electric vehicles (EVs). It covers parameters such as electrical performance, environmental conditions, safety, and life cycle assessment.
5. ISO 15194: This standard specifically addresses the lithium-ion batteries used in electric bicycles (e-bikes). It defines the performance and safety requirements for e-bike batteries, including their capacity, charging methods, and protection systems.
6. IATA Dangerous Goods Regulations: These regulations, developed by the International Air Transport Association (IATA), provide guidelines for the safe transport of lithium-ion batteries by air. They specify packaging, labeling, and documentation requirements to prevent the risk of fire or explosion during transportation.

## 4.8 Battery Management System

The charging of electric vehicles is composed of various components, which are gradually discussed in the "Basics of Electromobility" series. This article focuses specifically on the Battery Management System (BMS). The battery is the most expensive part of any electric car and if not properly handled, its lifespan can be significantly reduced and in unfavorable conditions, it can also pose a safety risk for the car and its occupants. The BMS is responsible for ensuring the correct conditions for each individual battery cell and therefore for the entire battery. In this article, we will briefly cover the design of batteries, the ideal external environment for optimal battery performance, and the design of the BMS, its main functions, and the main challenges in creating an effective BMS system.

### 4.8.1 BMS Construction

The BMS design is largely based on the battery design and is composed of a battery monitoring integrated circuit (BMIC), a cell management controller (CMC), and a battery management controller (BMC). The BMIC keeps track of individual battery cells and must immediately communicate any changes or issues to the CMC or BMC, so that they can respond in real-time and address any potentially hazardous situations. For instance, if the BMIC detects a battery cell overheating, it must send this information to the BMC promptly, which must then

make a quick decision on how to handle the situation, potentially shutting down the overheated cell if necessary.

The performance and response time of the BMS depend on the frequency of communication between the BMIC and the CMC/BMC. The more frequent the communication, the better the chance of successfully resolving any potential risks. However, it is challenging to design an effective communication network in an electric car due to electrical noise. Apart from monitoring, the BMS also includes circuits that balance the energy loads of different cells, to prevent problems from arising. This is crucial and will be discussed in more detail later. Depending on the complexity of the electric car, multiple microcontrollers may be added to monitor and control various tasks. Each BMS must be able to monitor not only the battery but also itself and must be able to differentiate between real and false alarms.

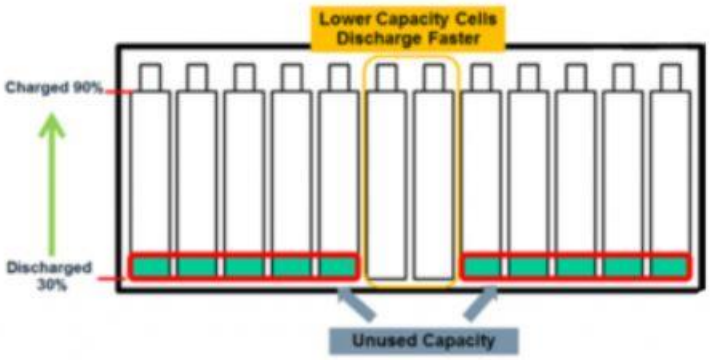


*Figure 4-3 Battery Capacity limits*

### 4.8.2 Basic Functions of BMS

The functions of a Battery Management System (BMS) are crucial to ensuring the proper functioning of a battery. To summarize, these functions include:

- **Charge and discharge control:** During AC charging, the on-board charger is responsible for converting AC current to DC, which is then sent to the battery in the required voltage. In the case of DC charging, the electric current goes directly to the BMS, which controls the charging and communicates with the DC station. The BMS must be intelligent, as the parameters of the battery change over time and the charging must adapt to these changes in real time.

- **Determination of the State of Charge (SOC):** This function is essential in determining how much longer the driver can drive. Determining the SOC is complicated, as it is affected by many variables such as temperature and current load. As accurate measurement is not possible, the SOC is based on computer battery models, which are estimates.

- **Determination of State of Health (SOH):** The SOH is defined as the ratio of the current full capacity to the full capacity of the battery at 0 kilometers. Battery health is affected by many factors, including temperature, charging current, and number of charging cycles. However, determining battery health precisely is difficult, so approximate computer models are used that take into account various variables.

- **Power balancing:** Cell balancing is a mechanism used in battery management systems to ensure that each cell in a battery pack is charged and discharged evenly. In a battery pack, each cell has a slightly different capacity and internal resistance, which can cause the cells to become unbalanced over time. This imbalance can lead to reduced performance, lower efficiency, and can even cause safety issues in extreme cases. Therefore, cell balancing is an essential mechanism to maintain the health and performance of a battery pack [18].

  There are various methods of cell balancing, including passive balancing, and active balancing. Passive balancing is the simplest method and most economical one. Passive balancing involves using a resistor to dissipate excess energy from the highest charged cells to be equal to the lowest charged cells. On the other hand, active balancing transfers energy from the highest charged cells to the lowest cells using a balancing circuit [22].

  One of the challenges in lithium-ion cell balancing is achieving a balance between performance and cost. Active balancing systems can be more effective than passive systems in maintaining cell balance, but they can also be more expensive and complex to implement. In contrast, passive balancing systems are simpler and more cost-effective, but they may not be able to maintain cell balance as effectively [21].

  Additionally, the use of lithium-ion batteries in electric vehicles and other high-power applications has driven the development of more advanced cell balancing systems which can further improve the performance and reliability of these batteries. Therefore, there is ongoing research in the area of cell balancing to develop more effective and efficient

techniques and algorithms to meet the growing demand for high-performance lithium-ion batteries and also to achieve a balance between performance and cost [19].

- **Recording and communication:** The BMS records and communicates information on the battery's characteristics, operation, and diagnostics. It communicates with other parts of the car, such as the on-board charger or charging station, and provides information to the driver on the car's charging status and distance traveled. The BMS also stores and processes the history of the battery's operation.

# 5 Literature Review

## 5.1 BMS Development

The development of a BMS system requires solving multiple challenges. Two of the most important challenges are Battery State Estimation and Battery Cell Charge Balancing. Battery State Estimation involves determining the state of charge of the battery, which is crucial information for both the driver and the system. There are three main methods for estimating the state of charge - the ampere-hour method, the open circuit voltage method, and model-based methods. The ampere-hour method is simple but prone to errors, the open circuit voltage method is accurate but can only be used when the car has been at rest for a long time, and model-based methods use both voltage and current measurements to estimate the state of charge. The use of intelligent algorithms, such as fuzzy logic and artificial neural networks, is also being explored.

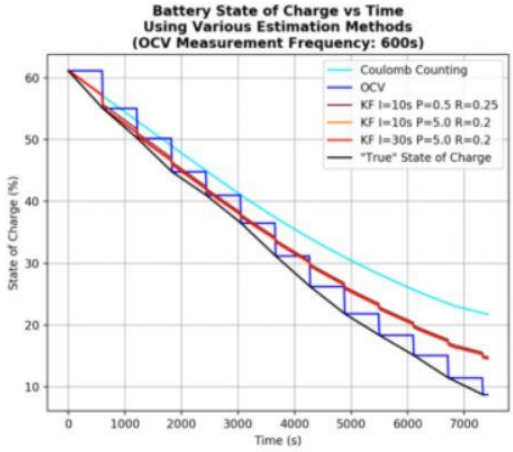


*Figure 5-1 Performance of different approaches for SOC estimation*

Creating computer models of batteries for charge level calculations is difficult because batteries are strongly nonlinear systems. There are two main approaches - electrochemical models and equivalent circuit models. The former is accurate but computationally complex, while the latter is widely used but less accurate. The goal of current research is to develop more accurate models or a combination of the current models that are less computationally demanding.

Battery Cell Charge Balancing is important to maintain performance and extend battery lifespan. Differences between cells can cause imbalances and reduce overall capacity. Passive

charge balancing methods discharge excess energy from cells with more energy, but this method wastes energy and complicates thermal control. Active charge balancing methods transfer energy between cells with the use of active switching circuits, but this requires more components and is more expensive. Different topologies are being explored to find the most efficient and cost-effective solution.

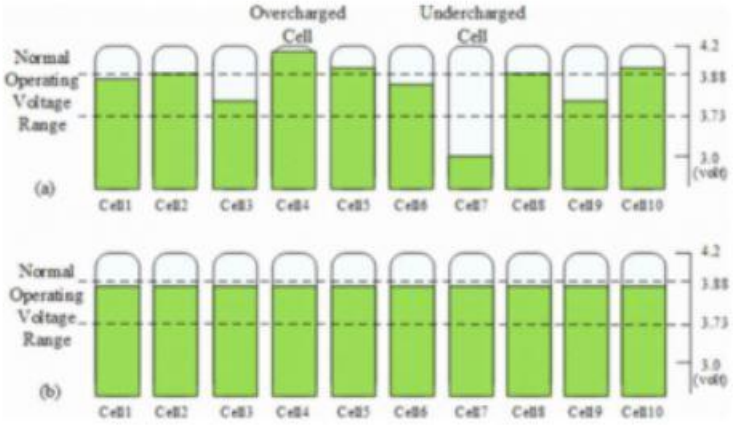


*Figure 5-2 Cell Balancing*

In conclusion, BMS is a crucial component of electric cars, protecting the battery from misuse and damage and ensuring it is ready for use. The design of a BMS system involves balancing cost, efficiency, and longevity, with a focus on ensuring security.

## 5.2 Battery Model

The battery model that needs to be developed for battery research should align well with the external features of the battery. The internal chemical reaction in the battery is a complicated non-linear process, and when charging and discharging currents change, the battery becomes polarized, meaning its terminal voltage does not have pure resistance characteristics, but instead changes in a non-linear way. This polarization results in an increase in the resistance of the charging and discharging current that flows through the battery. Over time, the battery may experience aging issues, such as a decrease in capacity and an increase in internal resistance, causing a serious deviation in the battery's state of charge. The power performance of the battery

is also reduced as it goes from a single battery component to a module to a pack, and these differences between batteries make it challenging to build an accurate battery model that can describe all battery performance. Therefore, various methods, such as electrochemical mechanism models, equivalent circuit models, and data-driven models, are used to simulate battery characteristics from different perspectives.

### 5.2.1 Electrochemical Model

The electrochemical mechanism model aims to describe the internal physical and chemical processes and external characteristics of a battery through establishing equations for electrochemical power and transmission. This considers the battery's internal mechanism, the physical and chemical properties of the positive and negative materials, the diffusion process, and electrochemical reaction. It mainly includes the pseudo-two-dimensional (P2D), single-particle (SP), and simplified pseudo-two-dimensional models (SP2D). The P2D model provides a rigorous and accurate depiction of the battery, but its complex equations make it difficult to solve in real-time for SOC estimation. The SP model is a simplified version of the P2D model that focuses on the main performance of the electrode and the influence of solid phase diffusion, but sacrifices accuracy. To improve its adaptability to high current conditions, the ESP model was developed based on the SP model and the P2D model was simplified to obtain other SP2D models. Reference [1] proposes a simplified multi-particle model that balances accuracy and complexity by using a predictor-corrector strategy and alignment, while Reference [2] improves the accuracy of SOC estimation through the SP2D-Iden model, which combines non-linear least squares method and Fisher information matrix analysis.

### 5.2.2 Equivalent Circuit Model

The equivalent circuit model is a method used to simulate the dynamic characteristics of batteries by using circuit components such as resistors, capacitors, and constant voltage sources. To accurately estimate the State of Charge (SOC) of the battery, the model must reflect both the static and dynamic characteristics of the battery, while not having an excessively high order, which would increase the computational requirements and make it more difficult to implement in practice.

The equivalent circuit model is divided into two categories: integer-order models and fractional-order models. Common integer-order models include the Rint model, Thevenin model, PNGV model, and multi-order model. The Rint model uses an ideal voltage source (Uoc) and the battery's internal DC resistance (R0) to describe the battery's dynamic characteristics, but this model is not suitable for applications in electric vehicles due to its low accuracy and failure to capture the polarization inside the battery.

The Thevenin model builds on the Rint model by adding a parallel RC network to simulate the polarization effect of the battery. It has a relatively simple structure and high simulation accuracy, and can effectively describe the abrupt and gradual changes in voltage that occur during battery charging or discharging. The Thevenin model requires fewer calculations in the subsequent estimation process, making it suitable for SOC estimation in embedded systems and electric vehicles.

The PNGV model is based on the Thevenin model and includes an additional capacitor in series to describe the change in battery open circuit voltage due to current integration during long-term charging and discharging. This model is nonlinear and has high accuracy in simulating the transient response process, making it suitable for large current and more complex charging and discharging conditions. However, it has a high level of complexity, requires a large amount of computation, and has low real-time performance.

Researchers have proposed various modifications to the PNGV model to improve its accuracy and performance. For example, reference [3] replaces the single RC circuit with a dual RC circuit to better characterize the polarization characteristics of the battery, while reference [4] sets R0, Rp, and Cp as variable parameters that change with the SOC to reduce complexity. Additionally, the multi-level RC equivalent circuit model contains multiple RC polarization parameters to describe the dynamic and static characteristics of the battery, but it becomes more difficult to identify the parameters as the number of RC components increases. Some researchers have proposed third-order equivalent circuit models that offer a balance of accuracy, complexity, and practical value, while others have proposed a hybrid model that combines different equivalent circuit models using the Bayesian method.

Ultimately, the choice of equivalent circuit model will depend on the specific requirements of accuracy and system reliability, as well as the available computational resources.

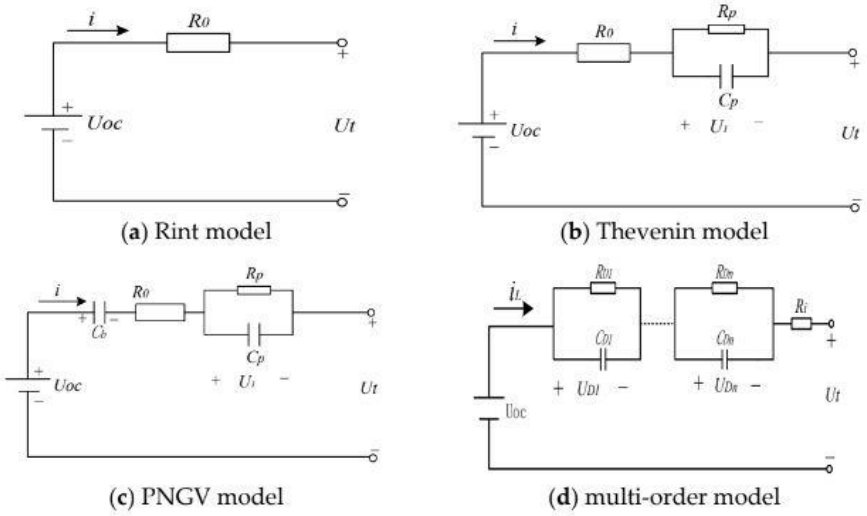


*Figure 5-3 Equivalent circuit for Battery*

## 5.2.3 Data-Driven Model

Data-driven models have gained immense popularity in recent times due to their versatility and the absence of the need for prior knowledge of the system being analyzed. These models can analyze the hidden information and the underlying rules of the system based on the external characteristic parameters of the system, bypassing the limitations of traditional modeling techniques that require model estimation and parameter identification. Data-driven models are widely utilized in battery modeling due to their high degree of non-linearity, self-learning capabilities, and good generalization ability, particularly in estimating the state of charge (SOC) of batteries in non-linear systems.

Data-driven models include various techniques such as neural network models, autoregressive models, and support vector machine models. These models do not require a clear model structure to simulate the internal reaction of the battery, and instead rely solely on sufficient test data to train the model, making it applicable to a wide range of battery types.

One example of a data-driven model for SOC estimation is the random forest regression model as proposed in reference [5]. This model effectively tackles the problem of over-fitting and improves the estimation accuracy, serving as a valuable reference for future research in this area. However, it is challenging to measure electrochemical parameters in real-life driving conditions due to frequent changes in operating conditions and large differences in energy consumption.

Reference [6] leverages vehicle energy consumption data and employs machine learning algorithms such as Lasso, Ridge, LGBoost, and XGBoost to train the data, thereby proposing a model for temperature stratified energy consumption. This model has a high level of accuracy and a good prediction performance. Another example is the radial basis function neural network model proposed in reference [7], which eliminates the impact of battery degradation on the accuracy of the original training model.

Despite the numerous advantages of data-driven models, they have some limitations, such as the need for a large amount of experimental battery data and the limitations in terms of estimation accuracy and versatility in cases where the number of data samples is small. Additionally, the algorithms used in these models can be computationally intensive and may not provide real-time performance, which poses a challenge for real-time applications, particularly in the case of electric vehicles.

# 6 Technical approach

## 6.1 State Of Charge

### 6.1.1 Assumptions

- The battery is perfectly isolated, so the thermal effect is not considered.
- The aging effect on the parameters is not considered, the drive cycle is for almost 11 hours which will not cause the parameters to change significantly, so That is a valid assumption.

### 6.1.2 Battery Modeling

To accurately represent a battery's characteristics, an excellent battery model must establish a balance between the complexity of the model and the battery's actual performance. The three main types of battery models are electrochemical, empirical, and equivalent circuit models. Due to the significant amount of computation required, electrochemical models—which are based on the electrochemical mechanism of the battery—are typically unsuitable for use as online estimators[14]. Empirical models, also known as the simplified electrochemical model, are developed by simplifying the electrochemical model. Equivalent circuit models are made up of fundamental circuit elements like resistors, capacitors, and voltage sources. They are widely used because of their low computational requirements and relatively straightforward mathematical structure[14]. By considering an appropriate trade-off between accuracy and complexity, the 3$^{rd}$ order equivalent circuit model for a Li-ion battery was selected as the battery model for this study as shown in Fig. 6-1. According to [15], a minimum of 3 RC pairs is needed to achieve a reasonable accuracy of battery representation

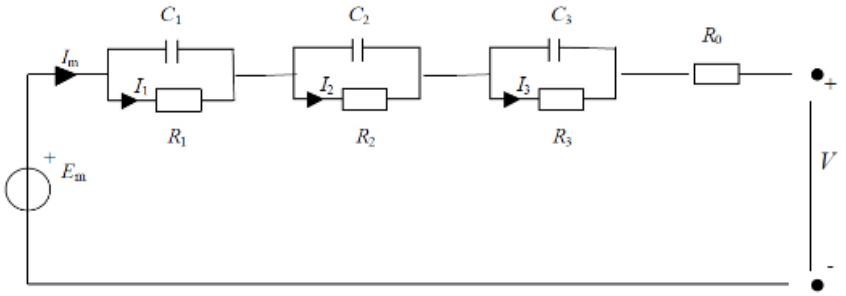


*Figure 6-1, Equivalent circuit representation of cell model* [2]

The state space formulation in discrete time domain is the following:

$$SOC(k) = SOC(k-1) - \frac{\Delta t}{Q_{nom}} I(k-1) + w_1(k-1)$$

*Equation 6-1 SOC equation*

$$V_1(k) = e^{-\frac{\Delta t}{\tau_1}} V_1(k-1) + R_1\left(1 - e^{-\frac{\Delta t}{\tau_1}}\right) I(k-1) + w_2(k-1)$$

*Equation 6-2 voltage at first RC branch*

$$V_2(k) = e^{-\frac{\Delta t}{\tau_2}} V_2(k-1) + R_2\left(1 - e^{-\frac{\Delta t}{\tau_2}}\right) I(k-1) + w_3(k-1)$$

*Equation 6-1 voltage at second RC branch*

$$V_3(k) = e^{-\frac{\Delta t}{\tau_3}} V_3(k-1) + R_3\left(1 - e^{-\frac{\Delta t}{\tau_3}}\right) I(k-1) + w_3(k-1)$$

*Equation 6-2 voltage at third RC branch*

Where *k* is a generic discrete time instant.

The first equation represents the $SOC$ dynamic, in which $Q_{nom}$ is the battery nominal capacity and $\Delta t$ is the discrete time step. The input current $I(k-1)$ is considered positive during discharging and negative during charging. The three RC parallels are used to model the dynamic response of the battery cell, and$\tau_1 = R_1 C_1$, $\tau_2 = R_2 C_2$ and $\tau_3 = R_3 C_3$ are the respective time constants. Those RC parallels can represent the charge transfer and diffusion phenomena inside the battery [16].$w(k)$ Represents the process noise.

The output equation of the model relates the average output voltage $V(k)$ of the cell model to the open circuit voltage $V_{OCV}$ and the voltage drops across the elements, as follows:

$$V(k) = V_{OCV}\big(SOC(k)\big) - V_1(k) - V_2(k) - V_3(k) - R_0 I(k) + v(k)$$

*Equation 6-3 Open-Circuit Voltage*

Where $R_0$ is the internal resistance of the battery and $v(k)$ represents the measurement noise.

The discrete time nonlinear state space model of the battery is written as:

$$x(k) = A\,x(k-1) + B\,u(k-1) + w(k)$$

$$y(k) = C\,x(k) + D\,u(k) + v(k)$$

*Equation 6-4 Non-Linear state space model of the battery*

$$x(k) = \begin{bmatrix} SOC(k) \\ V_1(k) \\ V_2(k) \\ V_3(k) \end{bmatrix} \quad A = \begin{bmatrix} 1 & 0 & 0 & 0 \\ 0 & e^{-\frac{\Delta t}{\tau_1}} & 0 & 0 \\ 0 & 0 & e^{-\frac{\Delta t}{\tau_2}} & 0 \\ 0 & 0 & 0 & e^{-\frac{\Delta t}{\tau_3}} \end{bmatrix} \quad B = \begin{bmatrix} -\frac{\Delta t}{Q_{nom}} \\ R_1\left(1 - e^{-\frac{\Delta t}{\tau_1}}\right) \\ R_2\left(1 - e^{-\frac{\Delta t}{\tau_2}}\right) \\ R_3\left(1 - e^{-\frac{\Delta t}{\tau_3}}\right) \end{bmatrix} \quad u(k-1) = I(k-1)$$

$$y(k) = V(k) \qquad C = [V_{OCV} \quad -1 \quad -1 \quad -1] \qquad D = -R_0$$

*Equation 6-5 State space model representation*

The state space equations and the measurement equation can also be represented as follows:

$$x(k) = f(x_{k-1}, u_{k-1}, w_{k-1})$$

$$y(k) = h(x_k, u_k, v_k)$$

### 6.1.3 Parameter Estimation

A power-oriented 31 Ah lithium ion cells of the $LiNi_xMn_yCo_zO_2$ (NMC) Chemistry [17] were tested at 20℃ temperature. All the discharging and charging schemes, and the experimental data were taken from [16]. The cell was initially charged to 100% and then subjected to partial discharge at 1C for 6 minutes as shown in Fig. 6-3. It was left to rest for 54 minutes till the voltage stabilizes so as to be considered a good estimate of the OCV as shown in Fig. 6-2. Every 1C discharge was equivalent to a 10% decrease in the SOC as shown in Fig. 6-4. The experiment determined the response of the cell to the current pulses, providing a mechanism to evaluate the parameters for the cell model.

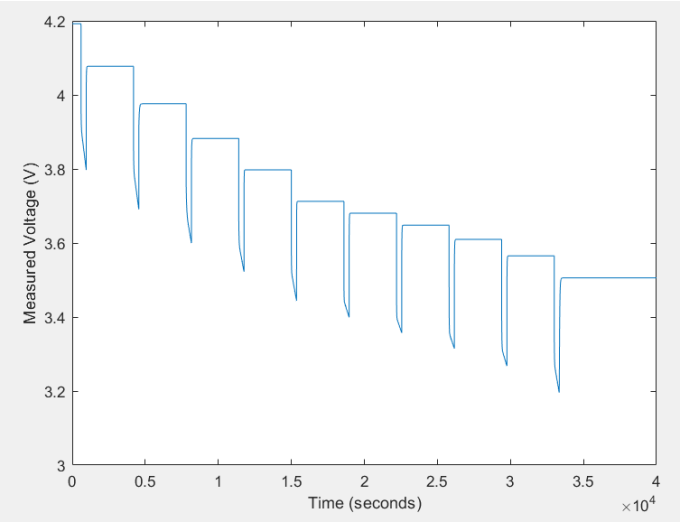


*Figure 6-3 OCV of the battery and ECM*

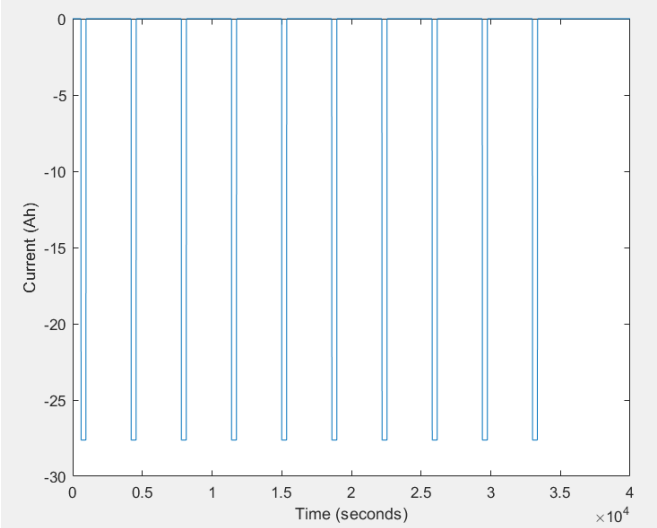


*Figure 6-2 Discharge pulses*

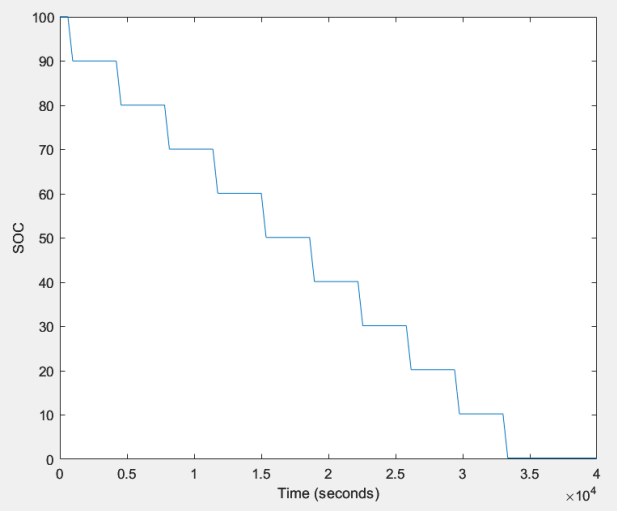


*Figure 6-4 SOC of the battery due to discharge pulses*

A parameter estimation stage and a simulation stage were included in the numerical analysis proposed here. A discharge profile was iteratively simulated and its outcomes were compared with experimental data during parameter estimation. The lookup tables for each circuit element were chosen to be based on 11 different points of SOC, with SOC breakpoints spaced by 10%, from 100% to 0%, to achieve a more accurate representation.

The Simulink Design Optimization parameter estimation tool was used to determine the parameters. The Simscape ECM was connected to a straightforward discharging circuit model using an ideal current source and a voltage sensor in order to enable the estimation, as shown in Fig. 6-5. Using the command line parameter estimation functionality, the estimation was automated. A set of one-dimensional lookup tables versus SOC for the eight parameters were generated from the pulse discharge curve at 20°C temperature. Simulink Design Optimization used Simscape to iteratively simulate the discharge profile while comparing the results of the simulation to experimental data in order to create these lookup tables. The algorithm of nonlinear least squares was employed to reduce the sum of squared errors by calculating the error gradient across all of the parameters. The flow diagram of Fig. 6-6. Illustrates the parameter estimation steps.

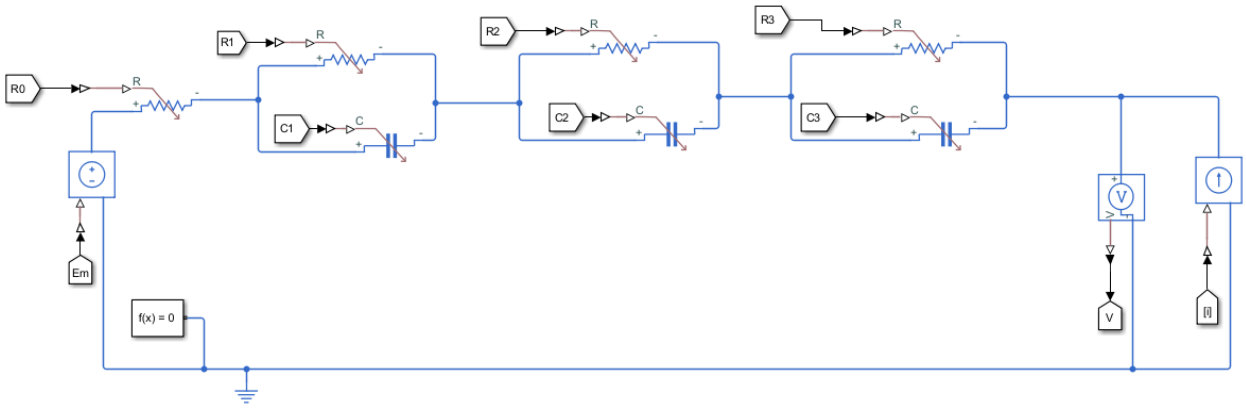


*Figure 6-5 Simscape model of ECM*

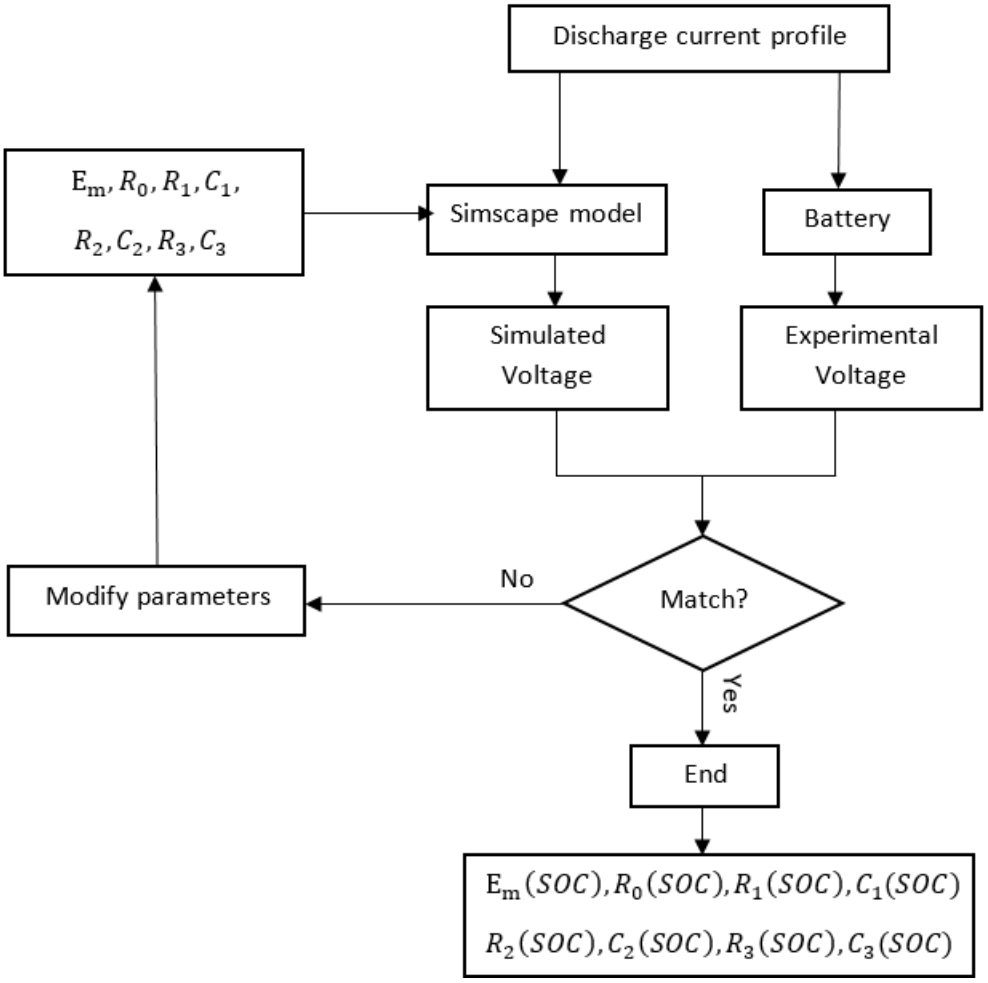


*Figure 6-6 Flow diagram of the parameter estimation procedures*

### 6.1.4 Unscented Kalman filter (UKF)

On the basis of OCV vs. SOC displayed in Fig. 6-7, SOC estimation is a nonlinear problem. Extended Kalman Filter (EKF) is frequently used for nonlinear estimation problems. However, the nonlinear functions are approximated by first-order or second-order terms of the Taylor series expansion. Thus, if the state space model is highly nonlinear, large errors are produced [18]. In this study, we utilized an unscented Kalman filter (UKF), which is accurate to the third order, in the sense of a Taylor series expansion for any nonlinearity. UKF adopts a nonlinear unscented transformation (UT) and a set of sample points, referred to as sigma points that are refreshed at each time step, to complete the recursion process. Those sigma points are generated according to the rule that their mean and covariance should be the same as expected mean and covariance of the system state, these points are transmitted through nonlinear model and then predictive points (including predictive state vector and system output) can be obtained. Finally, the mean and covariance of predictive points are revised to estimate the expected mean and covariance of

system state, in this way the posterior mean and covariance can be recursively transmitted according to the nonlinear mapping [19]

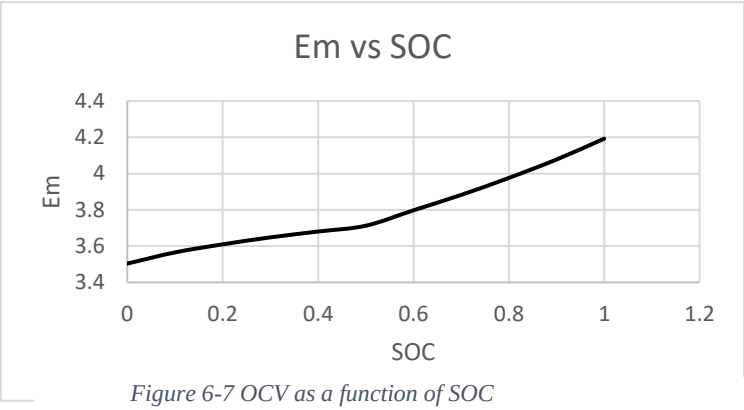


*Figure 6-7 OCV as a function of SOC*

Before the UKF recursion starts, an extended state vector needs to be constructed, model noise and measurement noise are included in this new state vector. According to battery state space model Eqs. 3.6, this extended state vector can be described as:

$$X = [x^T, w^T, v^T] = [SOC, V_1, V_2, V_3, w_1, w_2, w_3, v]^T$$

Assume that a Gaussian random variable $\boldsymbol{x}$ of dimension $L = 8$ has mean $\bar{\boldsymbol{x}}$ and covariance$\boldsymbol{P_x}$. Consider propagating $\boldsymbol{x}$ through the nonlinear function$\boldsymbol{y = g(x)}$. To calculate the statistics of $\boldsymbol{y}$, we first find a matrix $\boldsymbol{\mathcal{X}}$ of 2L + 1 sigma vectors $\boldsymbol{\mathcal{X}_i}$ with corresponding weights $\boldsymbol{W_i}$, according to the following equations [20]:

$$\boldsymbol{\mathcal{X}_0 = \bar{x}} \qquad \boldsymbol{i = 0}$$

$$\boldsymbol{\mathcal{X}_i = \bar{x} + \left(\sqrt{(L+\lambda)P_x}\right)_i} \qquad \boldsymbol{i = 1, \ldots, L}$$

$$\boldsymbol{\mathcal{X}_i = \bar{x} - \left(\sqrt{(L+\lambda)P_x}\right)_{i-L}} \qquad \boldsymbol{i = L+1, \ldots, 2L}$$

$$\boldsymbol{W_0^{(m)} = \frac{\lambda}{L+\lambda}} \qquad \boldsymbol{i = 0}$$

$$\boldsymbol{W_0^{(c)} = \frac{\lambda}{L+\lambda} + 1 - \alpha^2 + \beta} \qquad \boldsymbol{i = 0}$$

$$\boldsymbol{W_i^{(m)} = W_i^{(c)} = \frac{1}{2(L+\lambda)}} \qquad \boldsymbol{i = 1, \ldots, 2L}$$

Where$\boldsymbol{\lambda = \alpha^2(L+\kappa)}$. **L** is a scaling parameter, $\boldsymbol{\alpha}$ determines the spread of the sigma points around$\bar{\boldsymbol{x}}$, $\boldsymbol{\kappa}$ is another scaling parameter, and $\boldsymbol{\beta}$ is used to incorporate prior knowledge of the distribution of $\boldsymbol{x}$.

The estimated mean and covariance of *y* are computed by the weighted sample mean and covariance as follows:

$$\bar{\boldsymbol{y}} = \sum_{i=0}^{2L} \boldsymbol{W_i^{(m)} y_i}$$

$$\boldsymbol{P_y} = \sum_{i=0}^{2L} \boldsymbol{W_i^{(c)} (y_i - \bar{y})(y_i - \bar{y})^T}$$

The main steps of UKF are summarized as follows:

i) Initialize with $\widehat{\boldsymbol{X_0}} = \boldsymbol{E}[\boldsymbol{X_0}]$ and $\boldsymbol{P_0} = \boldsymbol{E}\left[\left(\boldsymbol{X_0} - \widehat{\boldsymbol{X_0}}\right)\left(\boldsymbol{X_0} - \widehat{\boldsymbol{X_0}}\right)^{\boldsymbol{T}}\right]$.

ii) For $k \in \{1, \ldots, \infty\}$, calculate the sigma points.

iii) State predication:

a. Propagate the sigma points through the state model:

$$\boldsymbol{\mathcal{X}_{k|k-1}} = \boldsymbol{f}\left[\boldsymbol{\mathcal{X}_{k|k-1}}\right]$$

b. Calculate the propagated mean:

$$\bar{\boldsymbol{X}}_{\boldsymbol{k}}^{-} = \sum_{\boldsymbol{i=0}}^{\boldsymbol{2L}} \boldsymbol{W_i^{(m)}} \boldsymbol{\mathcal{X}_{i,k|k-1}}$$

c. Calculate the propagated covariance:

$$\boldsymbol{P_k^-} = \sum_{\boldsymbol{i=0}}^{\boldsymbol{2L}} \boldsymbol{W_i^{(c)}}\left(\boldsymbol{\mathcal{X}_{i,k|k-1}} - \widehat{\boldsymbol{X}}_{\boldsymbol{k}}^{-}\right)\left(\boldsymbol{\mathcal{X}_{i,k|k-1}} - \widehat{\boldsymbol{X}}_{\boldsymbol{k}}^{-}\right)^{\boldsymbol{T}}$$

iv) Measurement update:

v) Propagate the sigma points through the measurement function:

$$\boldsymbol{y_{k|k-1}} = \boldsymbol{h}\left[\boldsymbol{\mathcal{X}_{k|k-1}}\right]$$

vi) Calculate the propagated mean:

$$\bar{\boldsymbol{y}}_{\boldsymbol{k}}^{-} = \sum_{\boldsymbol{i=0}}^{\boldsymbol{2L}} \boldsymbol{W_i^{(m)}} \boldsymbol{y_{i,k|k-1}}$$

vii) Calculate the estimated covariance:

$$\boldsymbol{P_{y_k^-, y_k^-}} = \sum_{\boldsymbol{i=0}}^{\boldsymbol{2L}} \boldsymbol{W_i^{(c)}}\left(\boldsymbol{y_{i,k|k-1}} - \bar{\boldsymbol{y}}_{\boldsymbol{k}}^{-}\right)\left(\boldsymbol{y_{i,k|k-1}} - \bar{\boldsymbol{y}}_{\boldsymbol{k}}^{-}\right)^{\boldsymbol{T}}$$

$$\boldsymbol{P_{x_k, y_k}} = \sum_{\boldsymbol{i=0}}^{\boldsymbol{2L}} \boldsymbol{W_i^{(c)}}\left(\boldsymbol{\mathcal{X}_{i,k|k-1}} - \bar{\boldsymbol{x}}_{\boldsymbol{k}}^{-}\right)\left(\boldsymbol{y_{i,k|k-1}} - \bar{\boldsymbol{y}}_{\boldsymbol{k}}^{-}\right)^{\boldsymbol{T}}$$

viii) Calculate Kalman gain $\boldsymbol{K}$ and update the state estimation and covariance:

$$\boldsymbol{K} = \boldsymbol{P_{x_k, y_k}} \boldsymbol{P_{y_k^-, y_k^-}^{-1}}$$

$$\bar{\boldsymbol{X}}_{\boldsymbol{k}} = \bar{\boldsymbol{X}}_{\boldsymbol{k}}^{-} + \boldsymbol{K}\left(\boldsymbol{y_k} - \bar{\boldsymbol{y}}_{\boldsymbol{k}}^{-}\right)$$

$$\boldsymbol{P_k} = \boldsymbol{P_k^-} - \boldsymbol{K}\boldsymbol{P_{y_k^-, y_k^-}}\boldsymbol{K^T}$$

## 6.2 State of Health

Working with a system based on chemical reactions puts restriction on the capabilities and the performance of the system as some properties fade with time which affect the performance of the system. Lithium-Ion batteries degrade with time as the number of irreversibility's in the reactions increases. Therefore, the health of the battery became a main criteria in measuring the performance of the battery and decide the feasibility of buying a new battery. The threshold for the health for most of the batteries used in the Electric vehicles is 80% which means when the capacity of the battery reach 80% of the rated capacity, the battery become highly inefficient, not feasible, and need to change.

This module aims to build an estimation procedure to estimate the state of health (SOH) of the LI-ion batteries using different techniques. The capabilities for the estimation is limited by the complexity of the batteries as the health of the battery could be represented only by an electrochemical model that can describe the chemical reactions and this process is complex enough since the results of the model is a partial differential equations cannot be solved analytically and it consume a lot of processing to be solved numerically. Also, the life-cycle of the batteries is not linear so it needs an accurate approach.

### 6.2.1 Working with Kalman filter.

The first approach for the estimation technique is to build a Kalman filter to estimate SOH. This technique is based to identifying the system states and build a state observer for the system to account for the dynamics of the system. This approach is mentioned in some research papers but the system and the state observer are not mentioned in any of them. Therefore, no references were found and can be used to validate or explain the details of the approach. This approach has been ignored and another approach have been used.

### 6.2.2 Experimental data

This approach is based on an experimental data used from experiments conducted by (Xu et al., 2018). The results of the experiments is used to investigate the correlation between the dependent and independent variables capacity retention and number of cycle's respectively. By a curve fitting technique, a polynomial equation for the data will be generated. The data mainly is produced from examine the performance of Lithium-ion battery using Dynamic stress test (DST).

The battery have been under standard conditions to minimize the errors and reduce the number of variables, so the tests were done with temperature of 20 C and constant humidity level.

The available capacity in the battery vary with the number of cycles could be found from this graph which is adapted from (Xu et al., 2018).

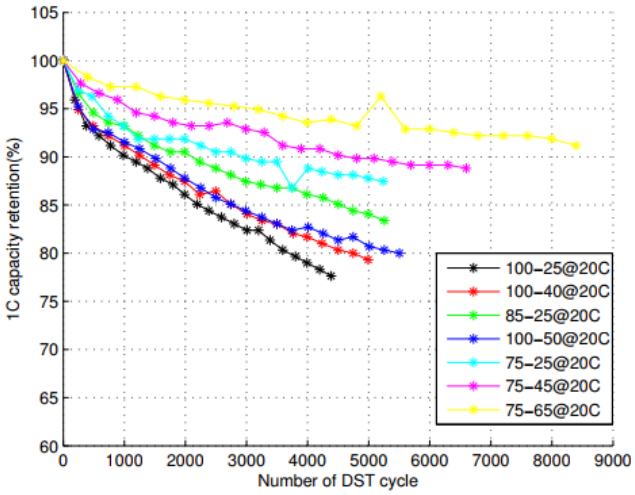


*Figure 6-8 Available capacity verses number of cycles*

For simplicity purposes, the normal operational temperature is almost constant (20 C) and the normal range for charging and discharging is (25% : 85%) as this is the most convenient range as the battery should not be fully charged or fully discharged as this will reduce the life time and increase the losses of the battery.

MATLAB algorithm adopted from MATHWORKS has been used to extract the points in the graph and build the model (Andrea, 2023).

The algorithm adopted to calculate the number of cycles is sensitive to any change in the battery condition (charge, discharge) as any peak in the SOC profile is recorded and counted as a cycle. The adopted algorithm is mainly a logical procedure that compares the current SOC level with the previous one to detect any change in the slope of the curve, in other words, the algorithm calculates the slope of the SOC curve and check, if the slope is a positive value, the battery is charging and so increment the number of cycles by 1 (the previous slope should be negative so the battery was discharging).

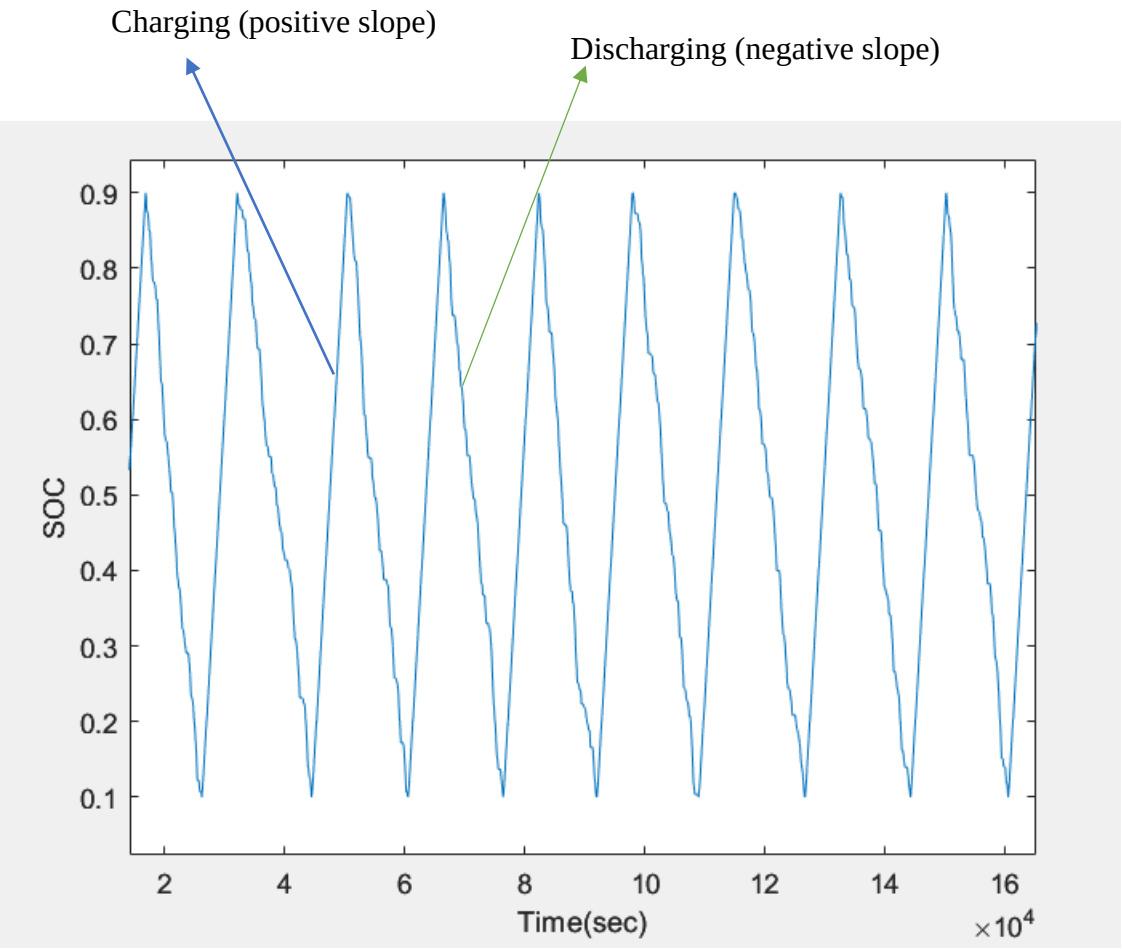


*Figure 6-9 counting cycles*

### 6.2.3 Flow chart

The graphical representation of the algorithm:

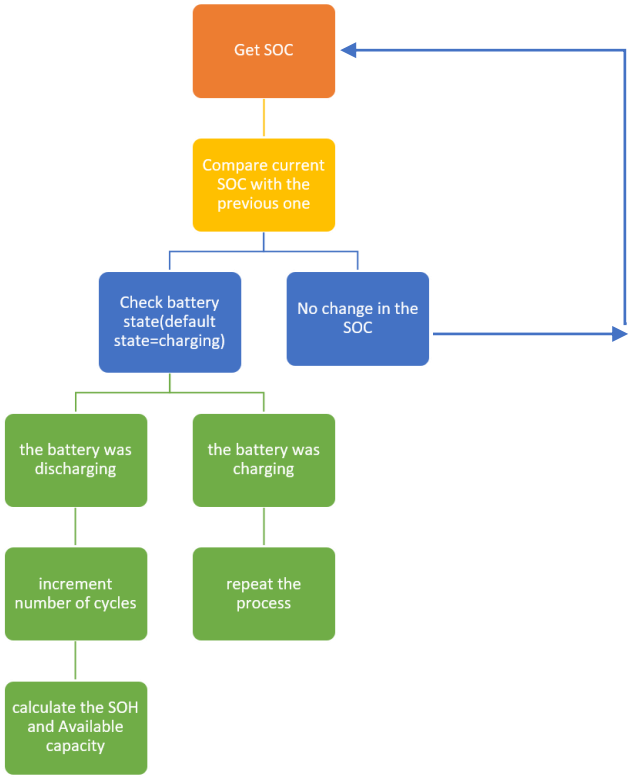


*Figure 6-10 algorithm graphical representation*

## 6.3 Cell Balancing

Energy efficiency is important for battery management and cell balancing systems, as it impacts how long the batteries can power applications. Achieving higher efficiency involves optimizing the design of the balancing system. In passive balancing systems, energy is wasted as heat through the bleeding resistors. The choice of resistor values and balancing current determines how much energy is dissipated. While a lower balancing current drains excess charge slowly, it leads to lower energy losses. In active balancing systems, energy is transferred between cells. The balancing current and time taken for charge transfer affect the overall efficiency. Though active balancing reuses the excess energy, some losses still occur during the charge transfer process. The balancing current is a crucial design parameter as it determines both the speed of balancing and amount of energy dissipated. Higher balancing currents balance cells faster but at the cost of more energy losses. In both passive and active balancing, optimizing the components and balancing current can improve the energy efficiency of the overall system, extending the usable life of the batteries. However, active balancing is generally more energy efficient since it redistributes rather than dissipates excess charge but needs more complex control [24].

To better demonstrate the balancing mechanisms. Three Simulink models were developed for simulating passive cell balancing, inductive active cell balancing and capacitive active cell balancing. The models allow studying the performance of the different balancing techniques in both charging and discharging modes.

The common components used in all three models include:

- A voltage source to charge the battery pack
- 4 battery cell models with different initial states of charge to represent an imbalanced battery pack
- MOSFET switches to enable/disable balancing circuits
- MATLAB Function blocks to implement balancing algorithms
- Powergui block for simulating the power electronics components
- Ideal switches to simulate charging and discharging modes

- Scopes to display time domain signals.
- Bus selector blocks to monitor individual cell voltages, SOC, and currents
- Diodes to control the current flow

Separate models were developed for charging and discharging modes to compare the performance of the different balancing techniques under both conditions. During simulations, the ideal switches would change position to activate either the charging or discharging circuit.

The key differences between the models lie in the balancing circuit components used:

- The passive balancing model uses bleeding resistors across each cell.
- The inductive active balancing model uses inductors to transfer charge between cells.
- The capacitive active balancing model uses capacitors to balance the cells.

The simulation results from the models allow studying and comparing the performance of passive, inductive active and capacitive active cell balancing techniques in terms of their ability to quickly equalize cell voltages and currents under both charging and discharging conditions.

### 6.3.1 Passive Balancing Model

Figure 3.101 shows four batteries with the same nominal voltage 3.7 V and nominal capacity 5.4 Ah with different SOC levels. Each battery is connected to the balancing circuit which consists of a mosfet and resistor of 1 ohm. There are two ideal switches, one is connected to the load and the other is connected to a DC voltage source to control the charging and discharging of the battery. The MATLAB function contains the control algorithm which simply dissipates the excess charges of the higher charged batteries to reach the same SOC of the lowest battery in the pack. The MATLAB function has the SOC of each battery as an input and the mosfet gate signal of each battery as an output.

### 6.3.2 Inductor Based Active Balancing Model

Figure 3.102 shows four batteries with the same nominal voltage 3.7 V and nominal capacity 5.4 Ah with different SOC levels. Each battery is connected to the balancing circuit which consists of two ideal switches, two diodes for each battery and a common capacitor of 10e-3 H. Each cell can be charged from the voltage source or from the inductor each has an independent circuit, and also can discharge its capacity to the load or to the inductor.

There are two ideal switches, one is connected to the load of 1 ohm and the other is connected to a DC voltage source to control the charging and discharging of the battery. The matlab function contains the control algorithm. It has 6 inputs. 4 of them are the SOCs of the batteries and the others are connected to 2-level PWM generators to control the ideal switch's signal. It has 8 outputs connected to the ideal switch signals input gates to control on and off time as the algorithm. The algorithm is focused on the battery with the highest SOC and the one with the lowest SOC. It works to transfer the charges from the highest SOC battery to the inductor then transfer the charges from the inductor to the lowest SOC battery.

### 6.3.3 Capacitor Based Active Balancing Model

Figure 3.103 shows four batteries with the same nominal voltage 3.7 V and nominal capacity 5.4 Ah with different SOC levels. Each battery is connected to the balancing circuit which consists of two ideal switches for each battery and a common capacitor of 100e-3 F. Each cell can be charged from the voltage source or from the capacitor, each has an independent circuit, and also can discharge its capacity to the load or to the capacitor. There are two ideal switches, one is connected to the load of 1 ohm and the other is connected to a DC voltage source to control the charging and discharging of the battery. The matlab function contains the control algorithm. It has 6 inputs. 4 of them are the SOCs of the batteries and the others are connected to 2-level PWM generators to control the ideal switch's signal. It has 8 outputs connected to the ideal switch signals input gates to control on and off time as the algorithm. The algorithm is focused on the battery with the lowest SOC. It works to transfer the charges from the whole pack to the capacitor, and when the capacitor is fully charged it transfers the charges to the lowest SOC battery.

The SoC of individual cells is adjusted through balancing, not the capacity imbalance. Just the balancing current has to be managed by the BMS. Unbalances must be adequately regulated in order to reduce the impact of cell voltage drifts. Every balancing strategy aims to increase the battery pack's usable capacity and enable the battery pack to run at the level of performance desired of it. Passive and active cell balancing algorithms utilize voltage balancing techniques. These algorithms examine whether the voltage difference between any two cells surpasses a threshold value. In a passive system, excess energy is dissipated through a balancing resistor, while in an active system, an inductor transfers excess energy to cells with low energy levels. To optimize the balancing thresholds, the accuracy of the sampling circuit can be improved, and the system requirements can be considered [8]. Passive balancing is the ideal choice for customers who want to save costs and adjust for long-term mismatches in self-discharge current.

## 6.4 Charging and Discharging Control

### 6.4.1 Bidirectional DC-DC Converter

Bidirectional DC-DC converters are an essential component of many power conversion applications, such as battery energy storage systems, electric vehicles, and renewable energy systems. These converters provide a way to transfer power bidirectionally between two DC power sources, such as a battery and a grid, or between two batteries. In this article, we will discuss the operation and design of bidirectional DC-DC converters, and the advantages and limitations of different topologies.

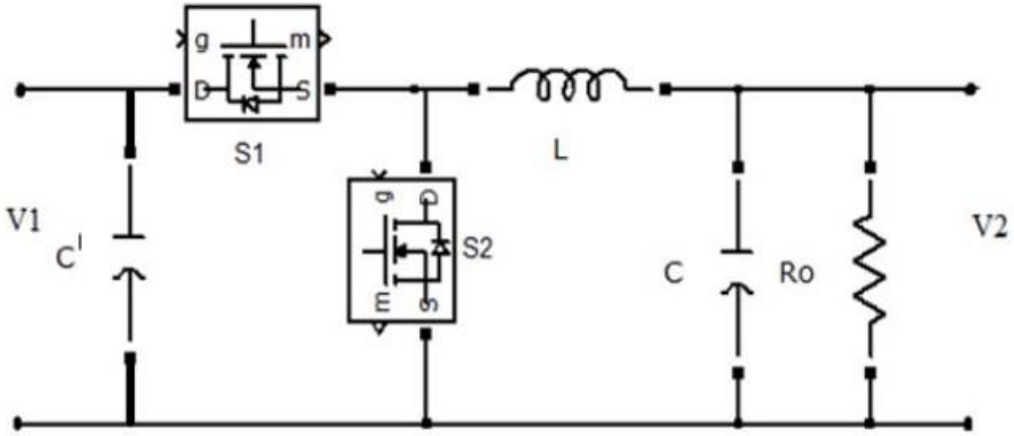


*Figure 6-11 Bidirectional DC-DC Converter*

Bidirectional DC-DC converters can transfer power in either direction, from the input to the output, or from the output to the input. The direction of power flow is determined by the voltage levels at the input and output terminals. When the input voltage is higher than the output voltage, the converter operates in the step-down (or buck) mode, and when the output voltage is higher than the input voltage, the converter operates in the step-up (or boost) mode.

In a bidirectional DC-DC converter, the power flow can be reversed by changing the direction of the current through the converter. This is achieved by using a bidirectional switch, which can be either a MOSFET or an IGBT. The switch is controlled by a high-frequency PWM signal, which determines the duty cycle of the switch and thus the output voltage.

The design of bidirectional DC-DC converters requires careful consideration of several parameters, such as power rating, efficiency, voltage regulation, and control strategy. The choice

of converter topology depends on the specific application requirements, such as input and output voltage levels, power rating, and switching frequency. The following are different types of DC-DC converters:

- **Buck-boost converter:** The buck-boost converter is a popular topology for bidirectional power transfer, as it can operate in both buck and boost modes. This converter consists of two switches, two diodes, and an inductor. The switches are controlled by a PWM signal, which determines the duty cycle of the switches and thus the output voltage.

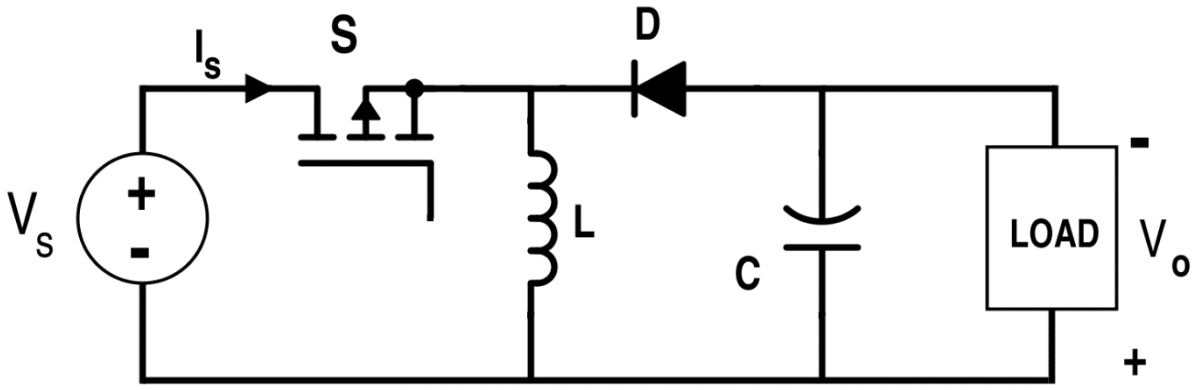


*Figure 6-12. Buck-Boost Converter*

- **Full-bridge converter:** The full-bridge converter is another widely used topology for bidirectional power transfer. This converter consists of four switches, which are arranged in a bridge configuration. The switches are controlled by a PWM signal, which determines the direction and magnitude of the output voltage.

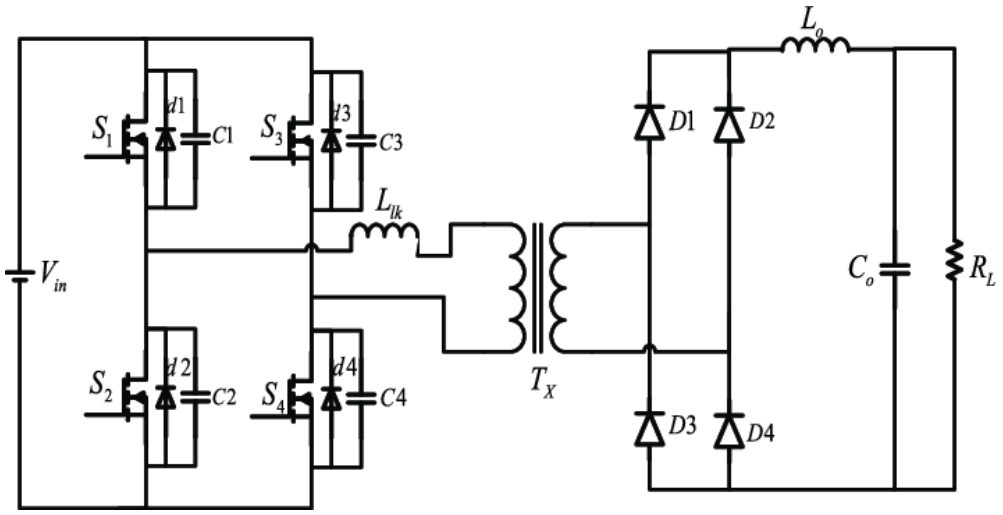


*Figure 6-13 Full-Bridge Converter*

- **Dual-active bridge converter:** The dual-active bridge converter is a high-frequency isolated bidirectional DC-DC converter. This converter consists of two full-bridge converters, which are connected by a high-frequency transformer. The transformer provides isolation between the input and output, and allows bidirectional power transfer.

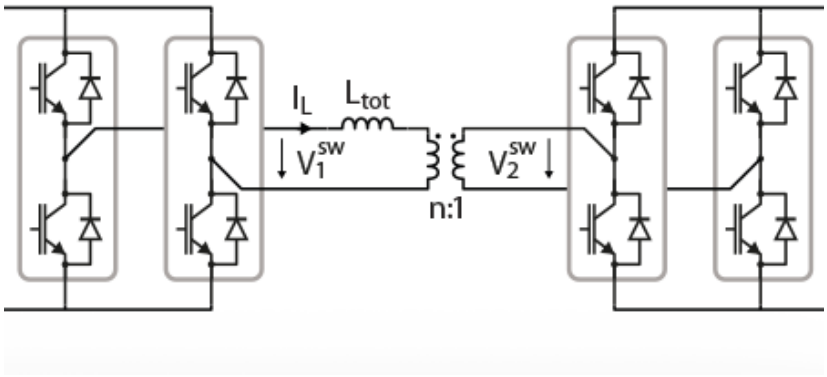


*Figure 6-14 Dual-active Converter*

One advantage of bidirectional DC-DC converters is their ability to transfer power bidirectionally between two DC power sources. This is particularly useful in applications such as battery energy storage systems, where energy can be stored from renewable sources and then discharged back to the grid when needed. Bidirectional DC-DC converters also play a critical role in electric vehicles, where they facilitate the transfer of power between the battery and the motor.

Efficiency is another important consideration in the design of bidirectional DC-DC converters. High efficiency is desirable in order to minimize power losses and maximize the overall system efficiency. This can be achieved by selecting the right converter topology, optimizing the component selection, and using advanced control strategies. For example, some bidirectional DC-DC converters use soft-switching techniques to reduce switching losses, while others use synchronous rectification to improve efficiency.

Another advantage of bidirectional DC-DC converters is their ability to provide voltage regulation. This is especially important in renewable energy systems, where the input voltage can vary widely depending on the source, such as solar panels or wind turbines. Bidirectional DC-DC converters can be designed to provide a stable output voltage, regardless of the input voltage, by using feedback control techniques.

However, bidirectional DC-DC converters also have some limitations, such as the need for careful design and control. The operation of bidirectional DC-DC converters can be complex, especially in high-power applications, and requires a thorough understanding of the underlying principles. Additionally, bidirectional DC-DC converters can be expensive to implement, especially in high-power applications where large components and complex control systems are required.

### 6.4.2 CCCV Charging Mode

The CCCV (Constant Current Constant Voltage) charging mode is a common charging mode used in bidirectional DC-DC converters for battery charging applications. This charging mode provides a two-stage charging process that helps to maximize the battery life and improve the charging efficiency.

In the first stage of the charging process, the bidirectional DC-DC converter operates in the constant current mode. During this stage, the converter provides a constant current to the battery, which helps to quickly charge the battery to a certain level. The charging current is typically set to a value that is safe for the battery and does not cause any damage or degradation. The constant current mode ensures that the battery is charged quickly and efficiently, without overheating or overcharging.

In the second stage of the charging process, the bidirectional DC-DC converter switches to the constant voltage mode. During this stage, the converter provides a constant voltage to the battery, while the charging current is gradually reduced. This stage helps to ensure that the battery is fully charged, while also preventing overcharging and overheating. Once the battery is fully charged, the charging process is stopped, and the bidirectional DC-DC converter can be switched to the discharge mode, where the battery can be used to power other devices.

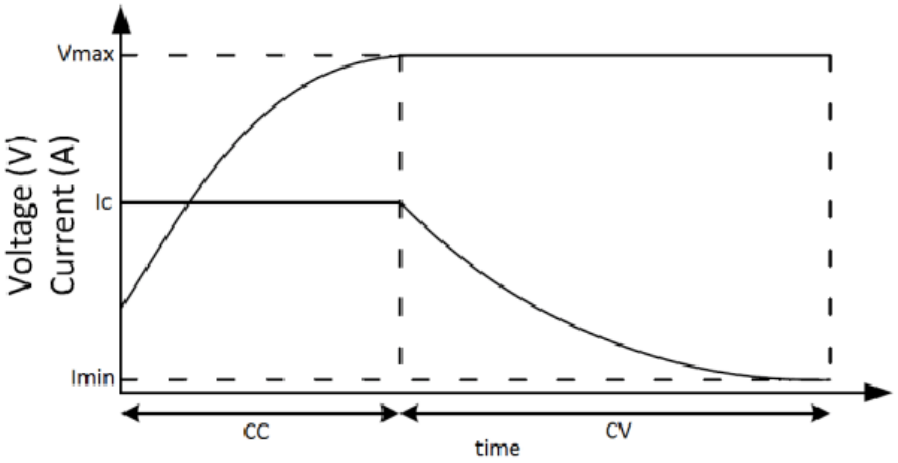


*Figure 6-15 CCCV Charging Method*

The CCCV charging mode is widely used in bidirectional DC-DC converters because it provides several benefits. Firstly, it helps to maximize the charging efficiency by ensuring that the battery is charged quickly and efficiently. This reduces the charging time and improves the overall performance of the system. Secondly, the CCCV charging mode helps to prevent overcharging and overheating, which can cause damage to the battery and reduce its lifespan. Finally, the CCCV charging mode can be easily integrated into the control system of the bidirectional DC-DC converter, allowing for precise control of the charging process.

Besides the CCCV charging mode, there are several other charging modes that are commonly used for lithium-ion batteries, depending on the application and the specific requirements of the battery. Some of these charging modes include:

- **Constant Current (CC) Charging:** In this charging mode, the charging current is kept constant throughout the charging process. This mode is typically used for fast charging applications, where the battery needs to be charged quickly. However, this mode can lead to overheating and overcharging if not controlled properly.
- **Constant Voltage (CV) Charging:** In this charging mode, the charging voltage is kept constant throughout the charging process. This mode is typically used for slow charging applications, where the battery needs to be charged slowly and gently. However, this mode can lead to undercharging if the charging voltage is not set correctly.
- **Trickle Charging:** In this charging mode, a low charging current is used to maintain the battery at a fully charged state. This mode is typically used for maintaining the charge of batteries that are not used frequently, such as backup batteries or standby batteries.
- **Pulse Charging:** In this charging mode, the charging current is applied in short pulses, with rest periods in between. This mode is typically used for rejuvenating batteries that have been discharged for a long time or have been left idle for a long time.
- **Fast Charging:** In this charging mode, a high charging current is used to quickly charge the battery to a certain level. This mode is typically used in applications where the battery needs to be charged quickly, such as electric vehicles or portable electronic devices.

Each of these charging modes has its own advantages and disadvantages, depending on the specific application and the requirements of the battery. The choice of charging mode depends on factors such as the battery chemistry, the charging time, the charging current, and the charging voltage, among others.

### 6.4.3 Discharging Mode

In addition to the charging mode, bidirectional DC-DC converters also have a battery discharging mode, which allows the battery to be used to power other devices or to feed energy back to the grid. The battery discharging mode is typically used in applications such as electric vehicles, renewable energy systems, and backup power systems.

In the battery discharging mode, the bidirectional DC-DC converter operates in the opposite direction to the charging mode, with the power flowing from the battery to the load or to the grid. The bidirectional DC-DC converter is designed to provide a stable output voltage, regardless of the battery voltage or the load current. The battery discharging mode is typically controlled by a feedback loop, which monitors the output voltage and adjusts the converter's duty cycle to maintain a stable output voltage. In some applications, the battery discharging mode may also be controlled by a microcontroller or a digital signal processor, which can implement advanced control algorithms to optimize the performance of the system.

One advantage of the battery discharging mode is that it allows the bidirectional DC-DC converter to provide a stable output voltage, even as the battery voltage changes over time. This helps to ensure that the load receives a consistent and reliable power supply, without any voltage fluctuations or dips. In addition, the battery discharging mode can be used to feed energy back to the EV using regenerative braking. This can help to improve the overall efficiency of the system, by reducing the amount of energy that needs to be stored in the battery.

Nevertheless, the battery discharging mode also has some limitations, such as the limited power capacity of the bidirectional DC-DC converter and the need for careful design and control. In high-power applications, the bidirectional DC-DC converter may need to be designed with larger components and more complex control systems, to ensure that it can handle the power requirements of the load.

# 7 Results

## 7.1 State of Charge

### 7.1.1 Parameter Estimation

The result of the parameter estimation procedure is presented in figures 7-1 to 7-7. These values constitute the look-up tables for the isothermal model. Figure 5, mentioned previously, shows how the e.m.f., represented here by the voltage source $E_m$, strongly depends upon the SOC. Figures 6-1 2show the variation of $R_0$, $R_1$, $R_2$, $R_3$, $C_1$, $C_2$ and $C_3$with state of charge.

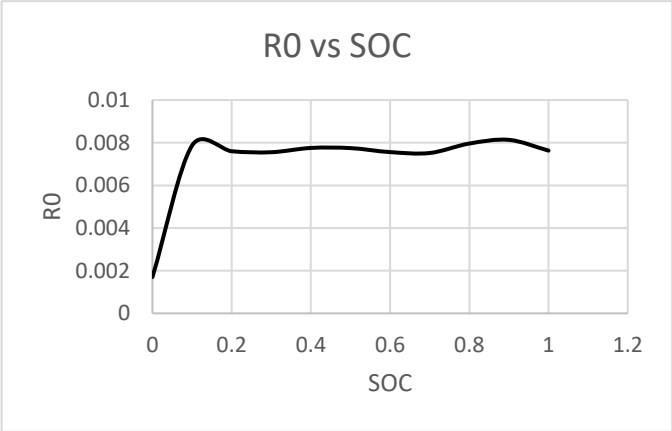


*Figure 7-1 internal resistance of the battery dependence on SOC*

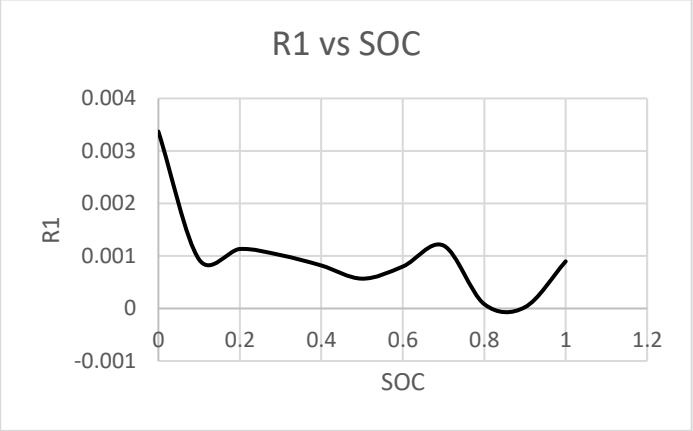


*Figure 7-2 Resistive component of the 1st RC pair dependence on SOC.*

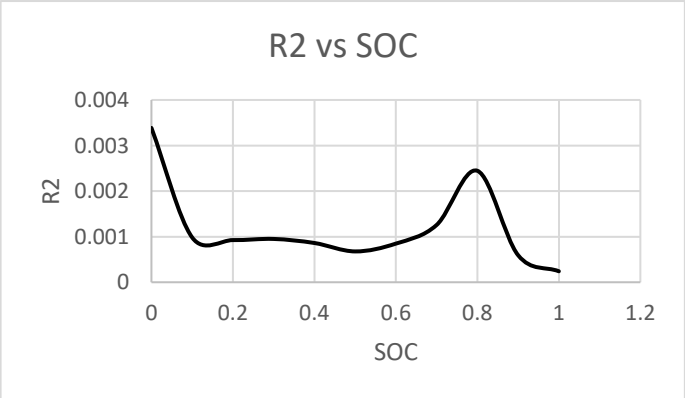


*Figure 7-3, Resistive component of the 2nd RC pair dependence on SOC.*

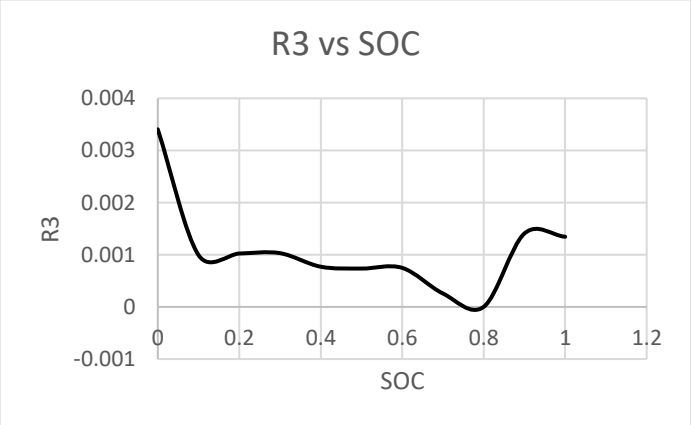


*Figure 7-4 Resistive component of the 3rd RC pair dependence on SOC*

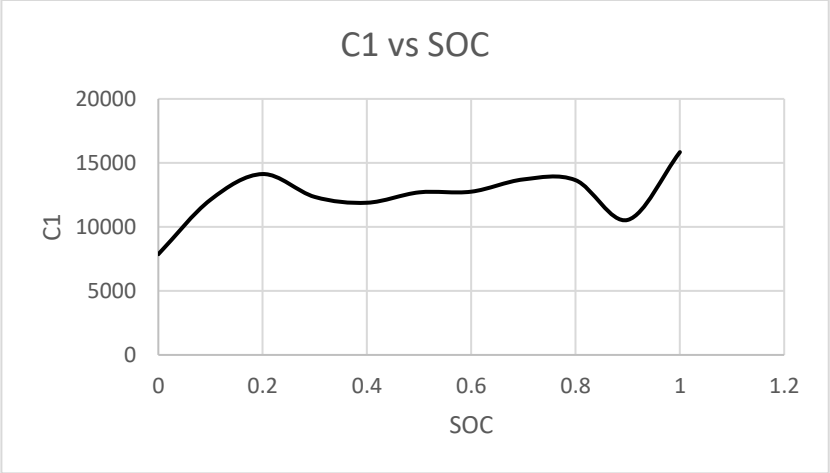


*Figure 7-5 capacitive component of the 1st RC pair dependence on SOC*

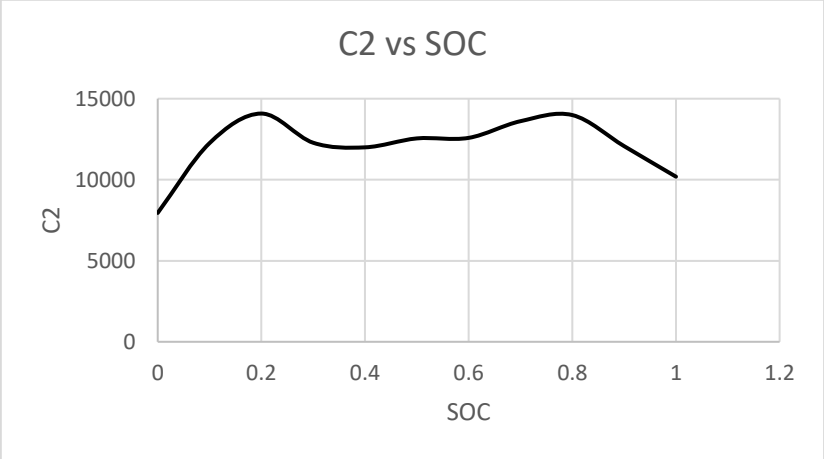


*Figure 7-6 capacitive component of the 2nd RC pair dependence on SOC*

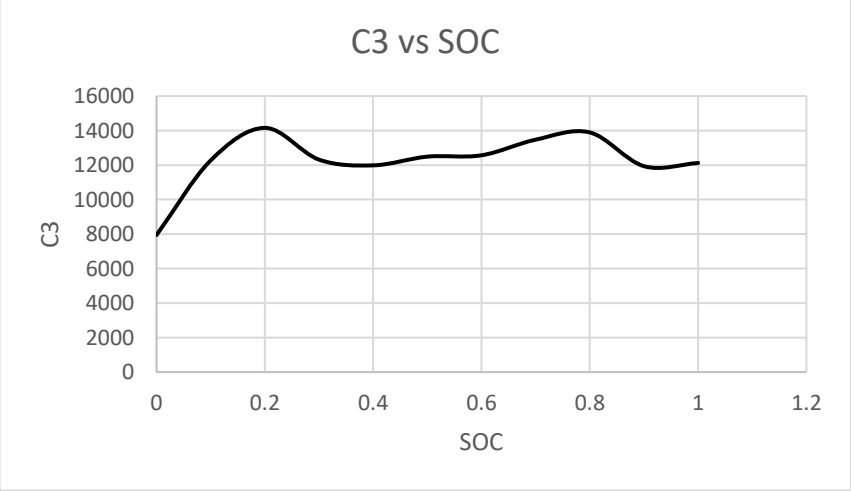


*Figure 7-3capacitive component of the 3rd RC pair dependence on SOC*

## 7.1.2 SOC Estimation

To verify the efficiency of the estimation, an actual drive cycle test is used. This drive cycle is composed of a combination of two EUDC drive cycles and two US06 drive cycles as shown in figures 7-8 and 7-9. US06 represents a city cycle and highway cycle with 8 miles route, an average speed of 48.4 mph, and 600 seconds duration. EUDC represents more aggressive driving modes with 10.85 miles route, an average speed of 20.7 mph, and 1190 seconds duration. The number of batteries used are 216 strings, 72S3P to produce 85 kW for the vehicle, Tesla PS85, used in the vehicle model to generate the current profile of the drive cycle.

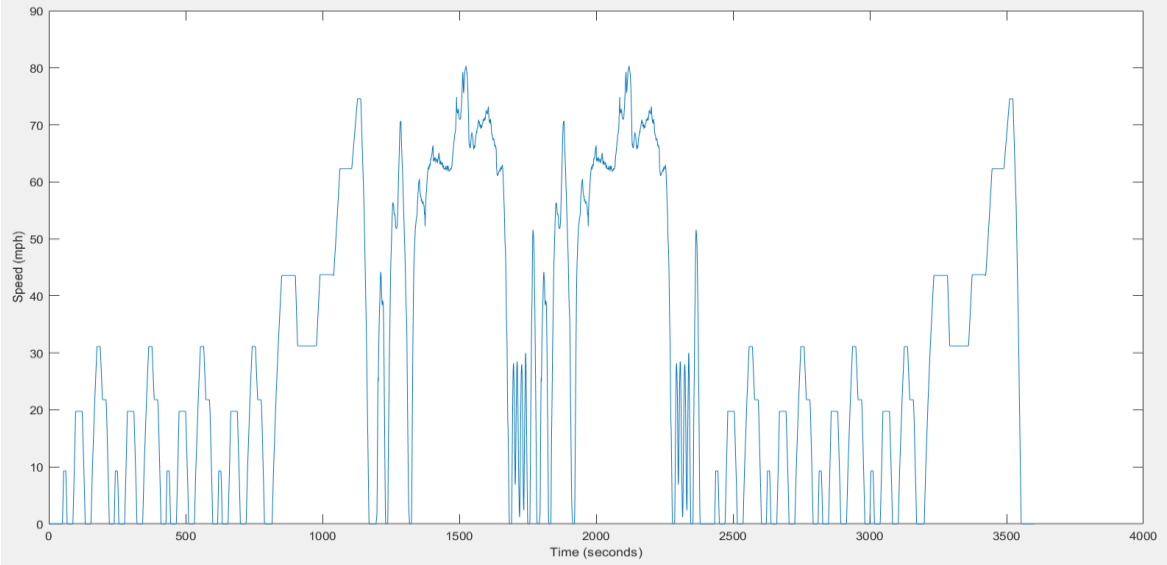


*Figure 7-8 Speed profile of the combined drive cycle*

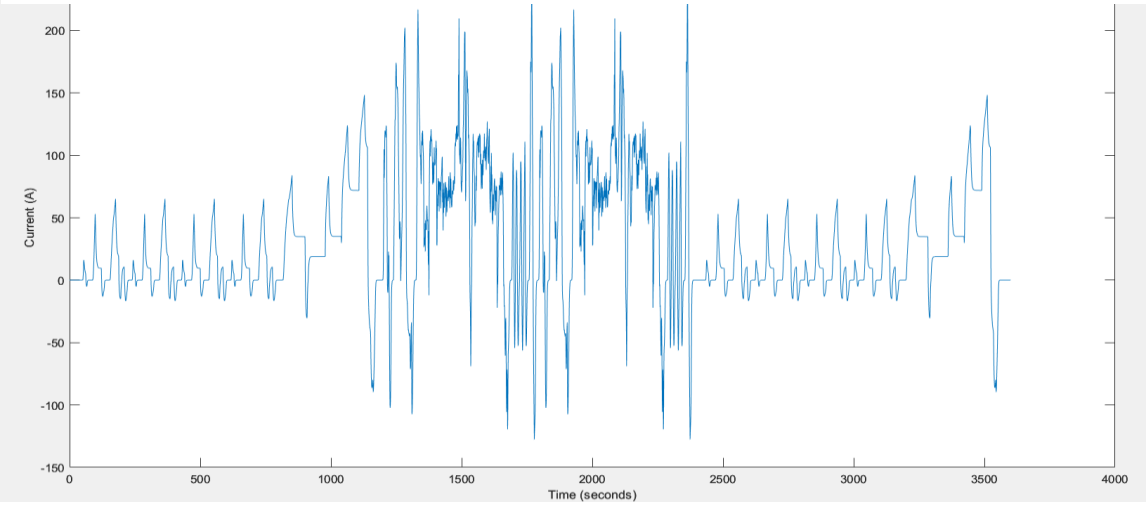


*Figure 7-9 current profile of the drive cycle*

The initial real SOC was set to 100%, while the initial estimated SOC was set to a different value to better evaluate the insensitivity of the proposed algorithm to the initial SOC estimate. The estimation results with the respective error are shown in figure 13.17. It can be shown that the simulation quickly compensated for the initial error. After correcting the initial errors, the estimated SOC converged to the real one after 2 seconds with 0% steady state error.


*Figure 7-4, Estimated SOC results with the error.*

## 7.2 State Of Health

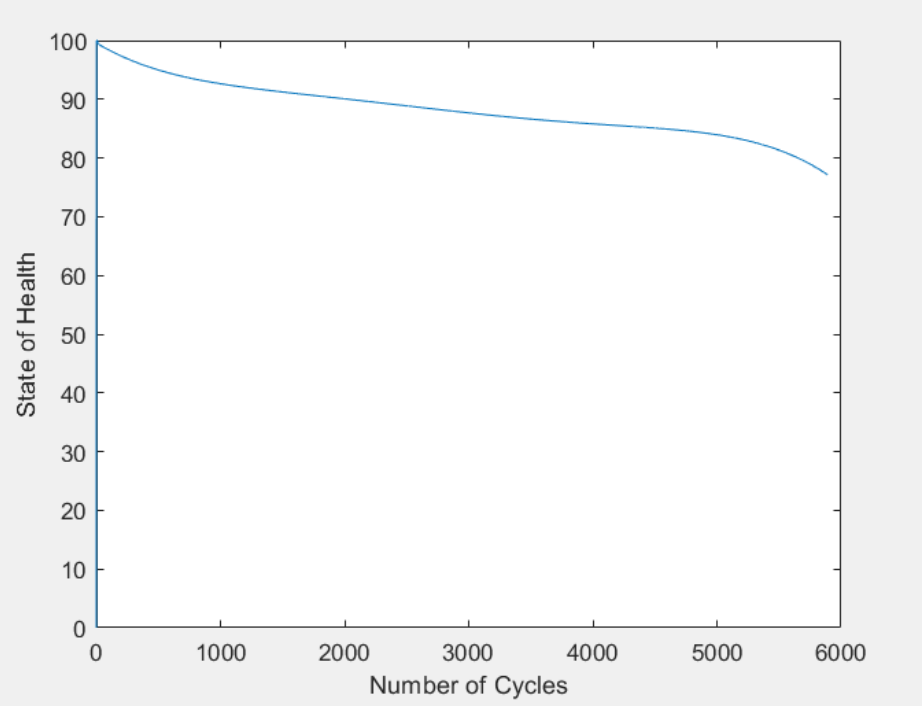


*Figure 7-5 State of Health for lithium-ion battery*

The curve fitting found to be 5th order as increasing the orders increasing the error of the fittings, the polynomial can be represented as follows:

$$y = -4.4410e^{-17}x^5 + 6.3175e^{-13}x^4 - 3.3763e^{-9}x^3 + 8.5540e^{-6}x^2 - 0.0127x + 99.5751$$

*Equation 7.1 Equation for the Experimental Data*

y: the percentage of the available capacity relative to the rated capacity.

x: number of cycles

The $R^2$of the fitted model is 0.991 which means that the independent variable can describe 0.991 of the variability in the dependent variable.

This equation will be used in the main model to have a live SOH mentoring as the SOC of the battery's changes.

Using MATLAB embedded function (`vpasolve`) to solve high order equations to find the expected number of cycles for the battery to reach 80% of its rated capacity, the required number of cycles is about 5651 cycle which is reasonable as the expected lifetime of the batteries is about 10 years. This high performance is for operation at 20 C (no thermal effects is included) and so under real life operations, this number of cycles will get reduced depends on many parameters such as the thermal effects, drive cycle, cooling system, etc.

## 7.3 Power Balancing

During the simulation, it was discovered that the passive balancer was significantly slower due to the higher voltage difference between the cells as shown in figure 3.104. However, this limitation of passive cell balancing can be addressed by utilizing active cell balancing. The power loss from passive balancing could be a major cause for the temperature rise near the battery pack, decreasing the battery life by stimulating the aging mechanisms. Capacitor-based active balancing requires less time than passive balancing as shown in figure 3.106, while inductor-based active balancing requires the least amount of time as shown in figure 3.105. Active cell balancing can achieve an efficiency of up to 95% compared to only 90% for passive cell balancing. However, active balancing topologies require more complex control than the simple control of passive cell balancing. Furthermore, passive balancing has a smaller size than active balancing topologies due to its simple components. As a result, the cost of implementation of passive cell balancing is much lower than active balancing topologies.

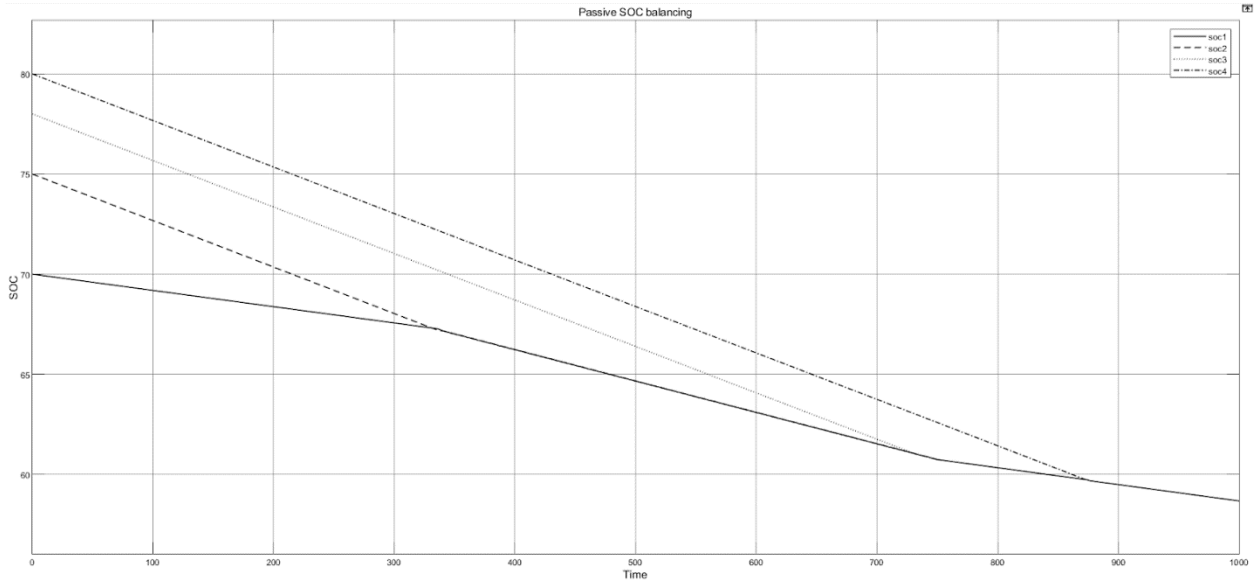


*Figure 7-6 Passive Balancing Discharging mode*

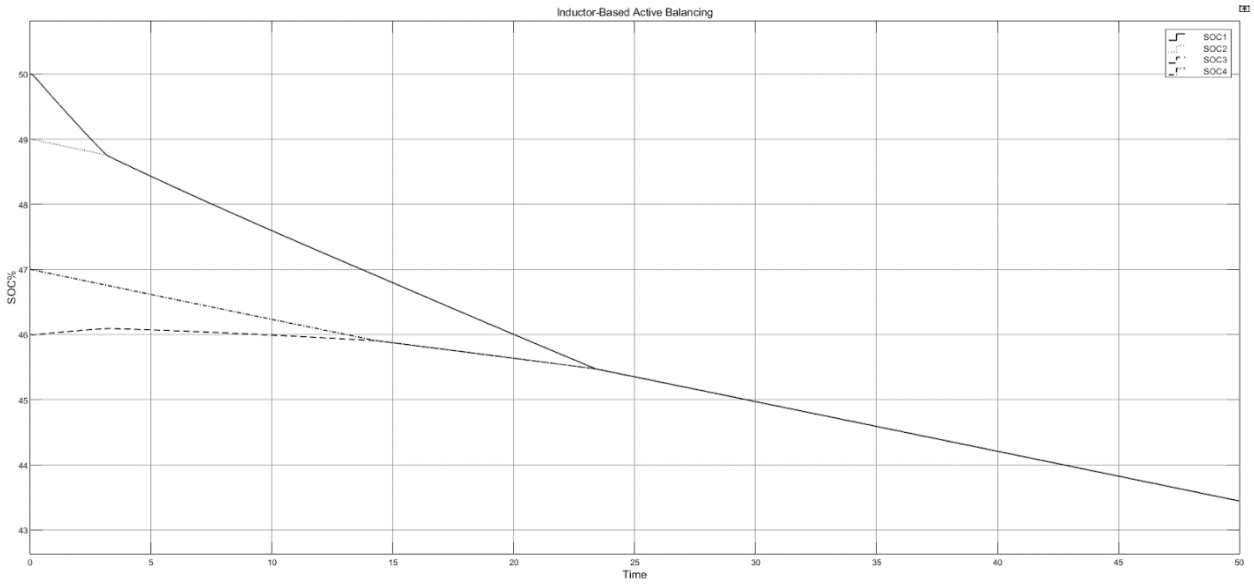


*Figure 7-8 Inductor based Active Balancing Discharging mode*

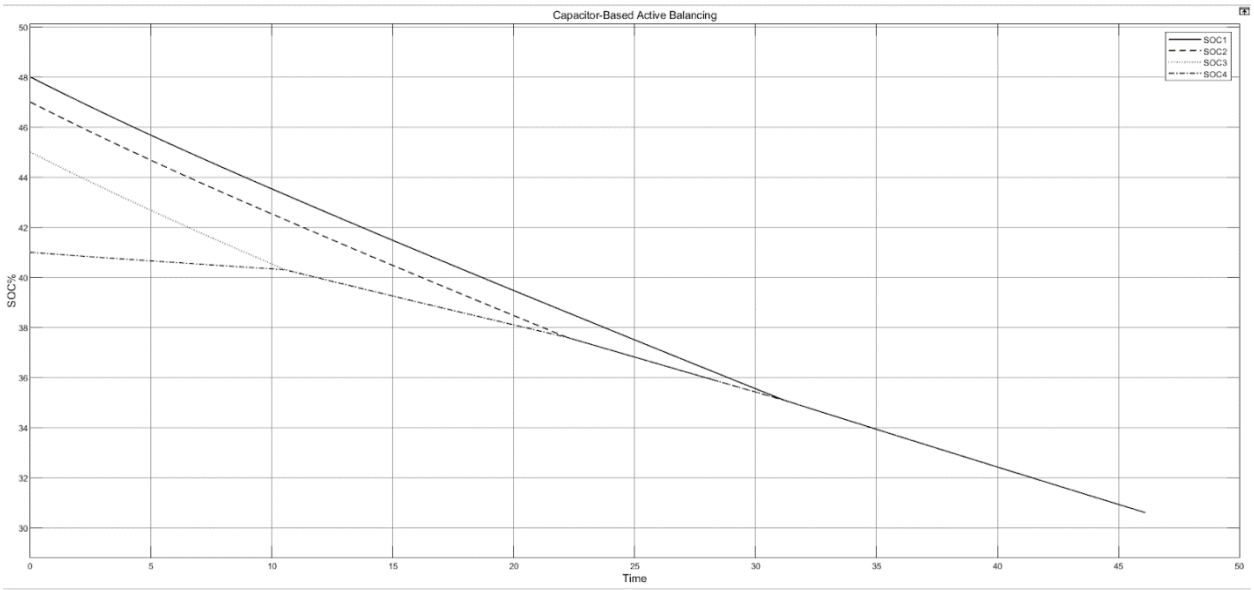


*Figure 7-7 Capacitor based Active Balancing Discharging mode*

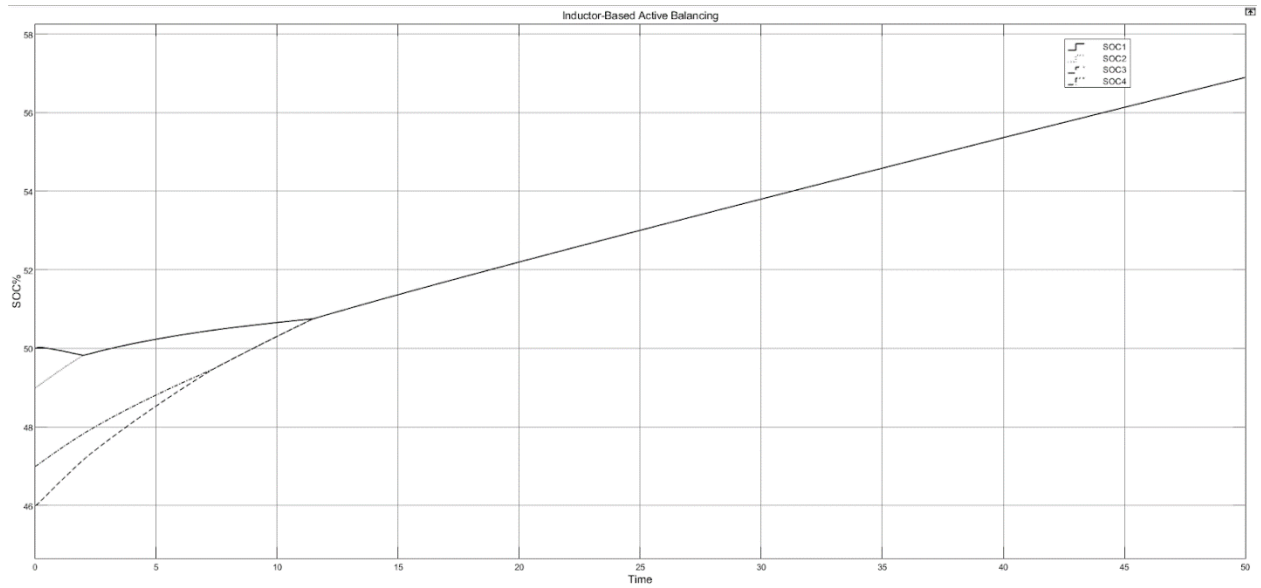


*Figure 7-10 Inductor based Active Balancing Charging mode*

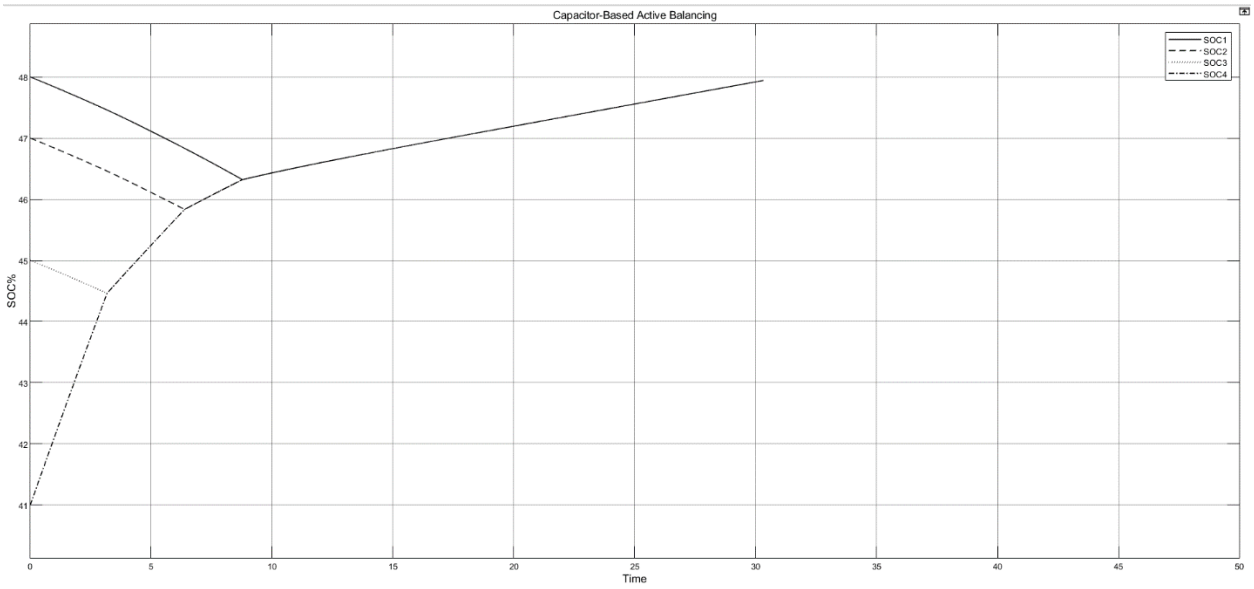


*Figure 7-9 Capacitor based Active Balancing Charging mode*

## 7.4 Charging and Discharging Control

### 7.4.1 CCCV Charging Mode:

Constant Current Phase:

- Initial SOC of the battery: 50 %
- Simulation Time: 200 s.

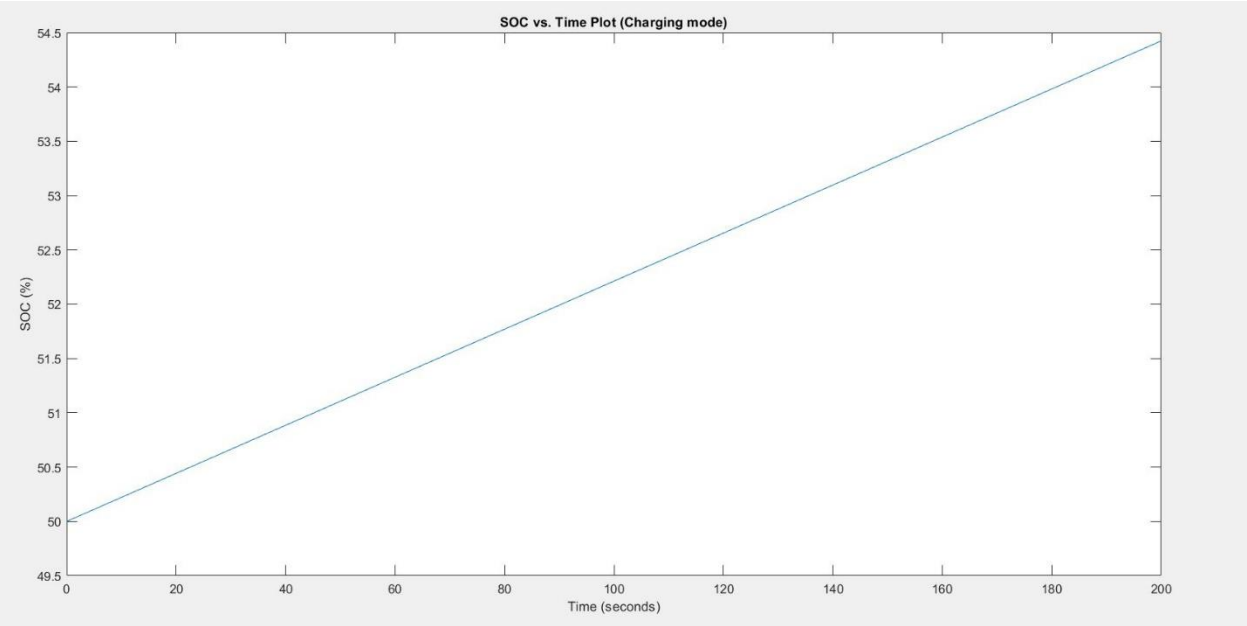


*Figure 7-11 State of Charge vs. Time Plot*

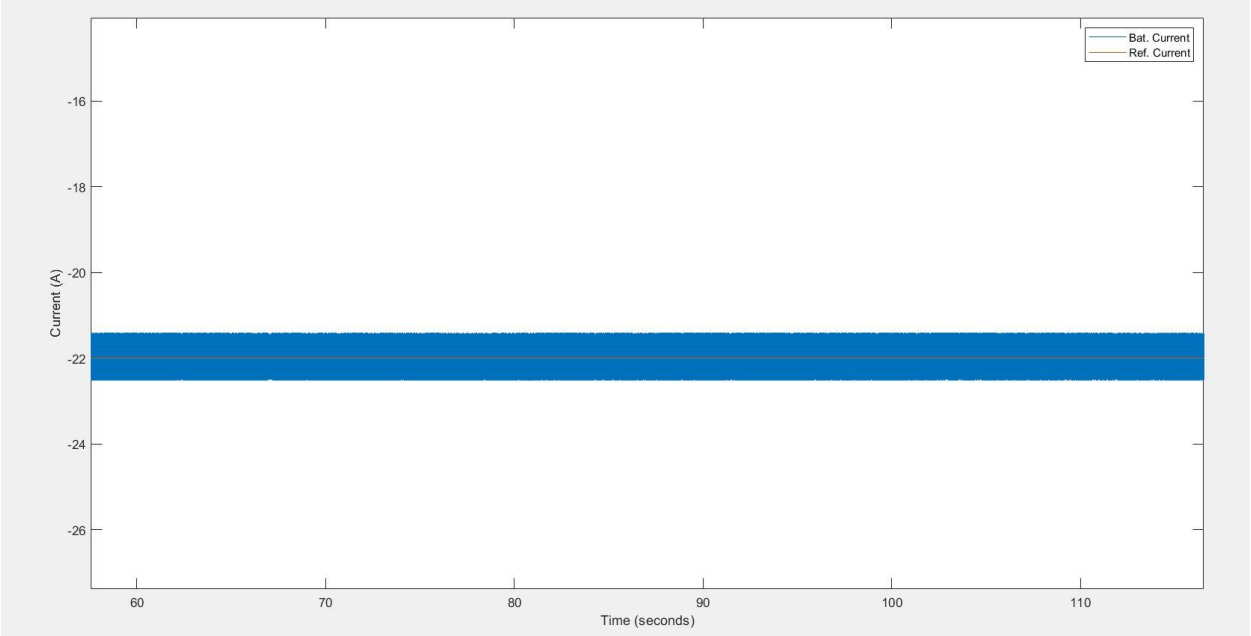


*Figure 7-13 Current vs. Time Plot*

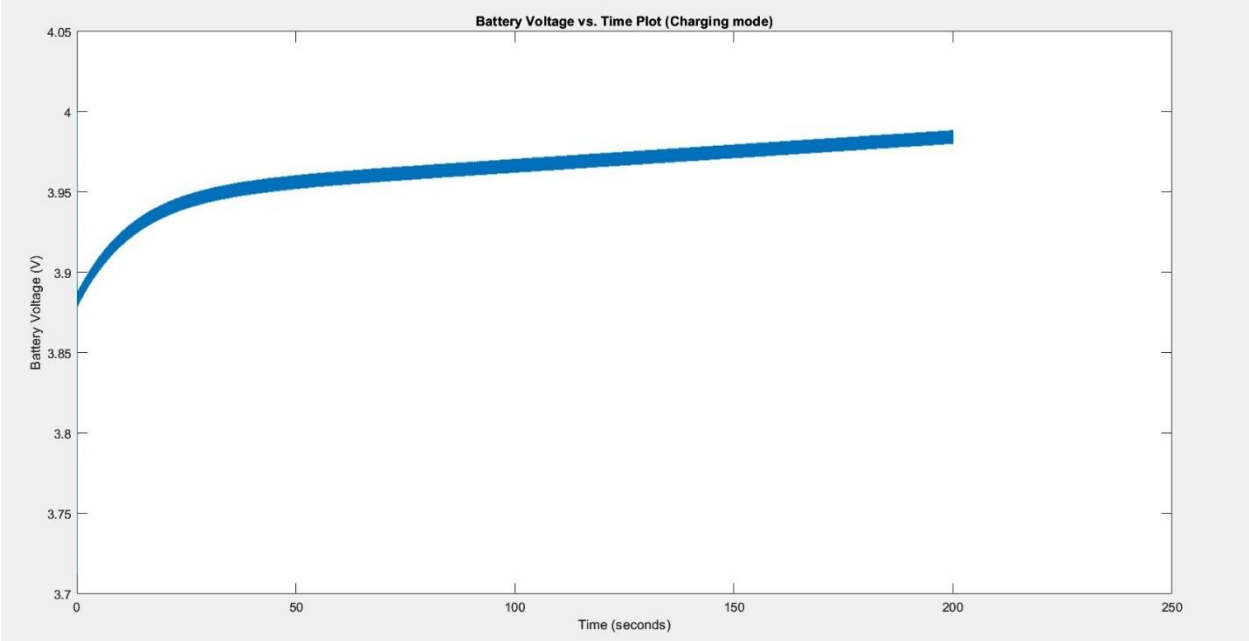


*Figure 7-12 Battery Voltage vs. Time Plot*

From the three plots above, it is clear that the battery is being charged from 50% to 54.5% SOC at a constant current (-22 A where the negative sign indicates that it is a charging current) while the battery voltage is increasing, and it will keep behaving the same until it reaches the 4.1 V value which corresponds to a 90% SOC. The control system is designed so that the charging mode stops once the SOC goes beyond 90% which corresponds to a theoretical 100% SOC for safety measures.

Constant Voltage Phase:

- Initial SOC of the battery: 91 %
- Simulation Time: 200 s.

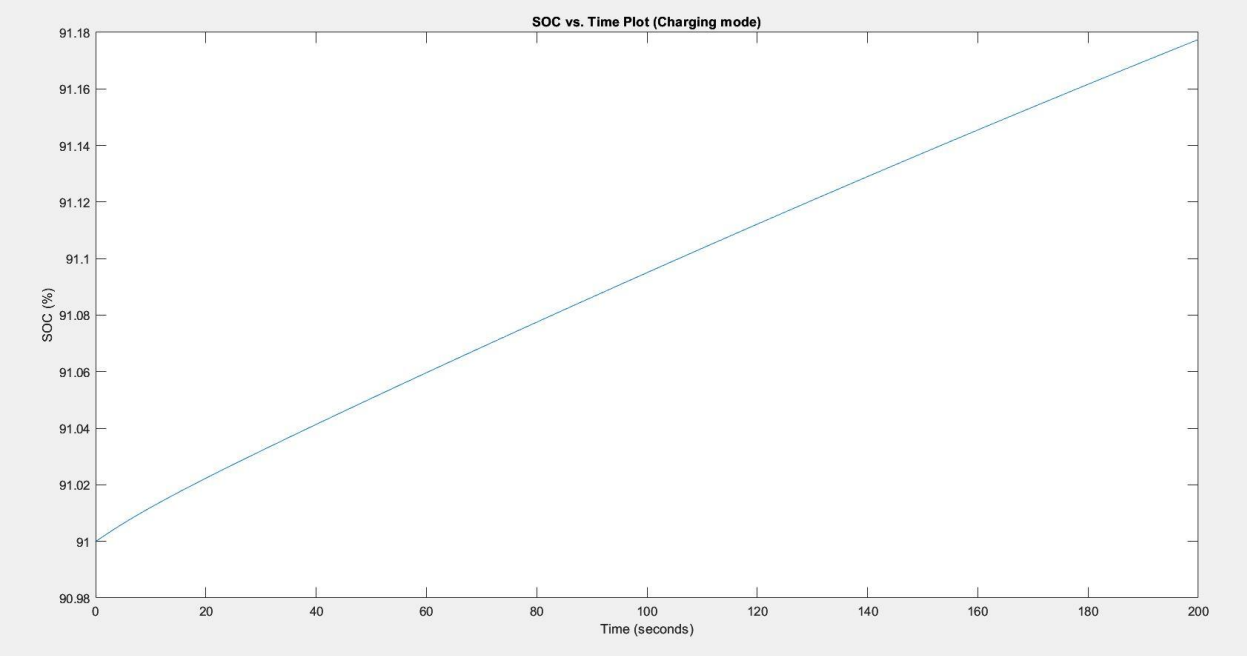


*Figure 7-14 State of Charge vs. Time Plot*

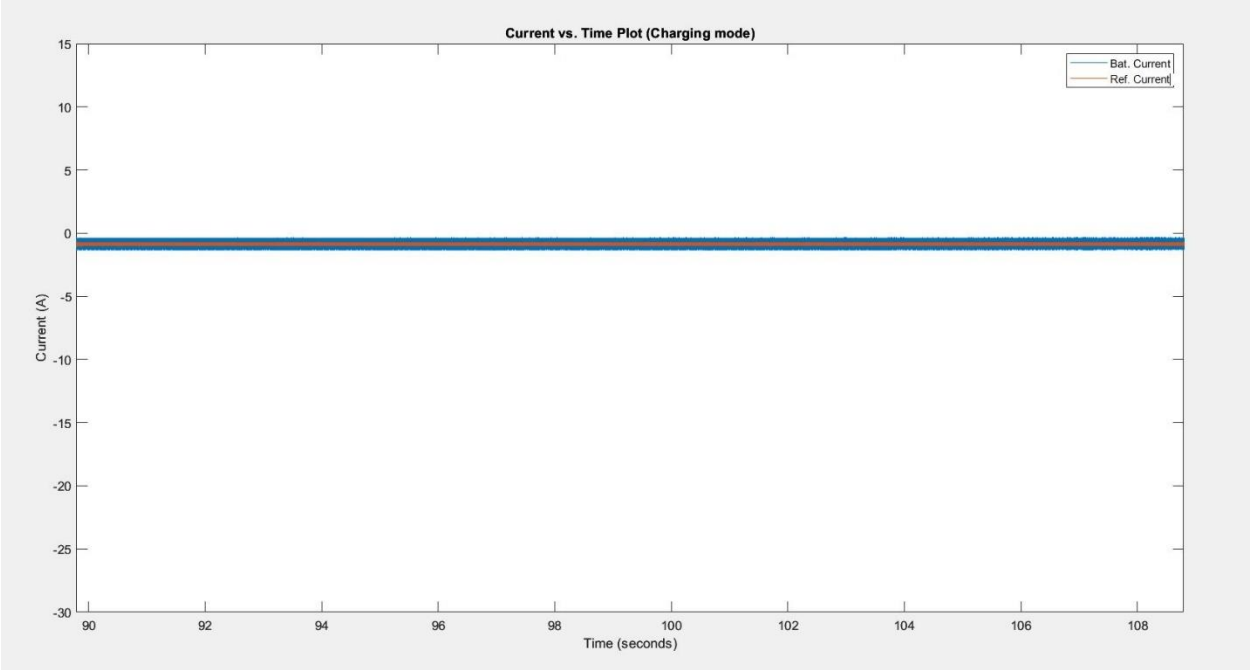


*Figure 7-16 Current vs. Time Plot*

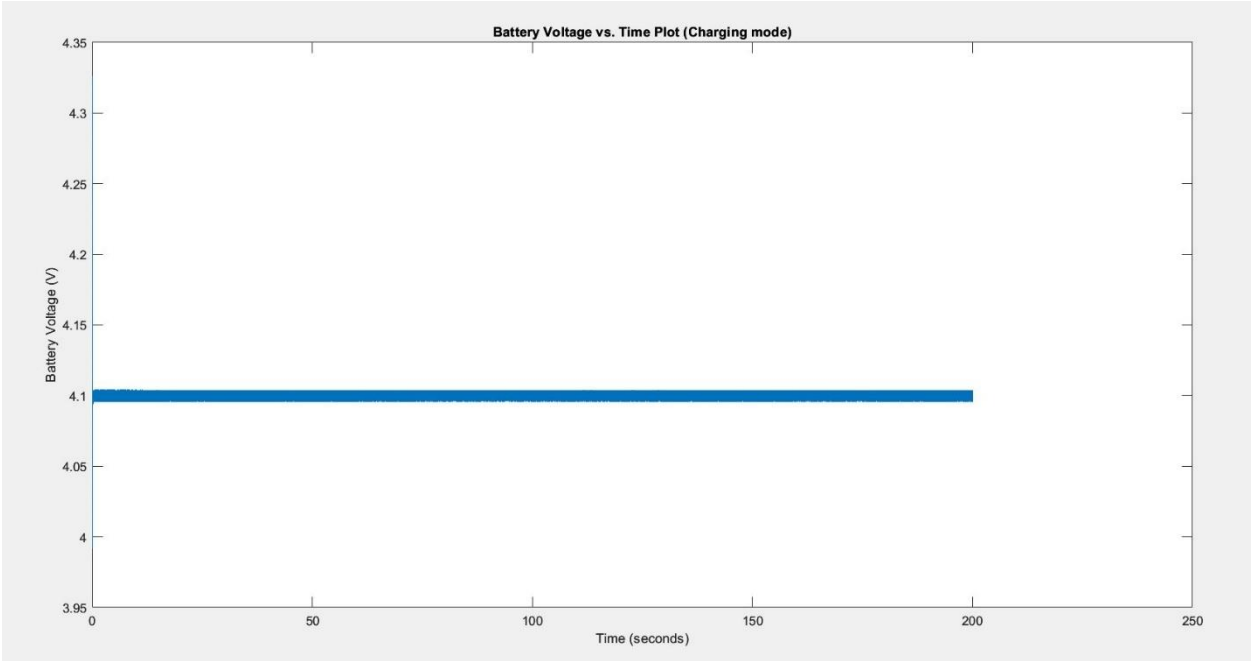


*Figure 7-15 Battery Voltage vs. Time Plot*

From the three plots above, it is clear that the battery is barely being charged as the SOC has only moved 0.18% up which isn't a significant number at all. The charging current drops down to around zero while the battery voltage is kept at a constant value of 4.1 which corresponds to a 90% battery SOC and a theoretical 100% SOC.

### 7.4.2 Discharging Mode:

- Initial SOC of the battery: 91 %
- Simulation Time: 200 s.

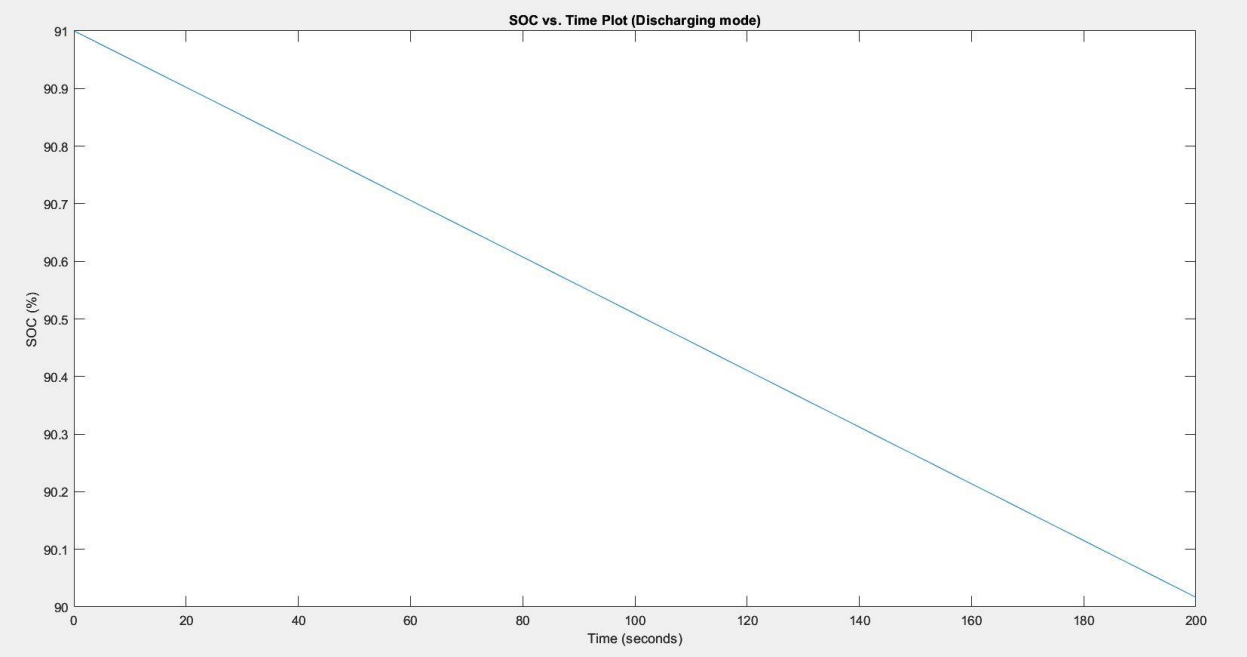


*Figure 7-17 State of Charge vs. Time Plot*

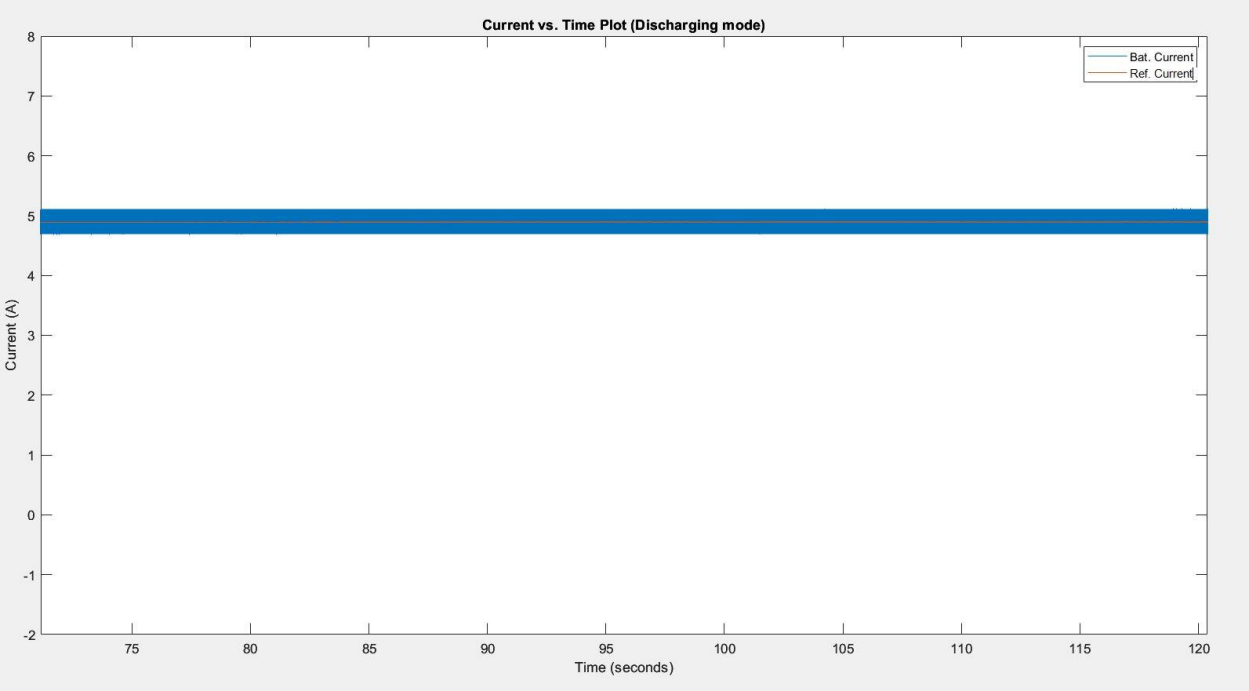


*Figure 7-19 Current vs. Time Plot*

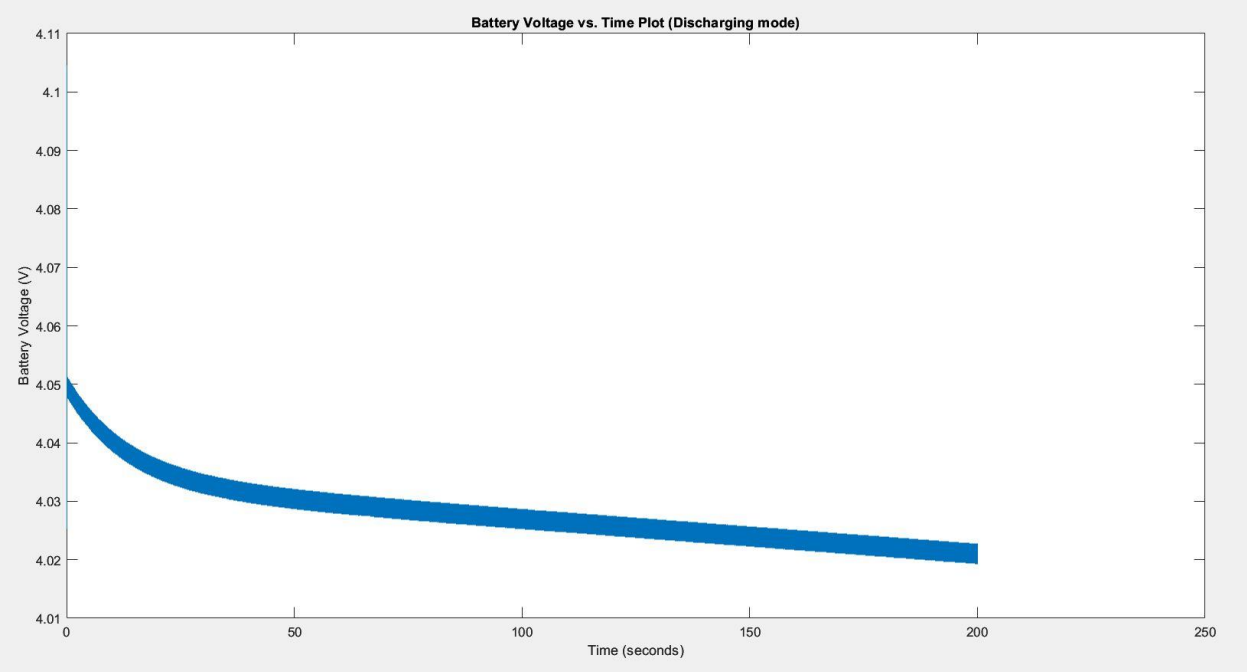


*Figure 7-18 Battery Voltage vs. Time Plot*

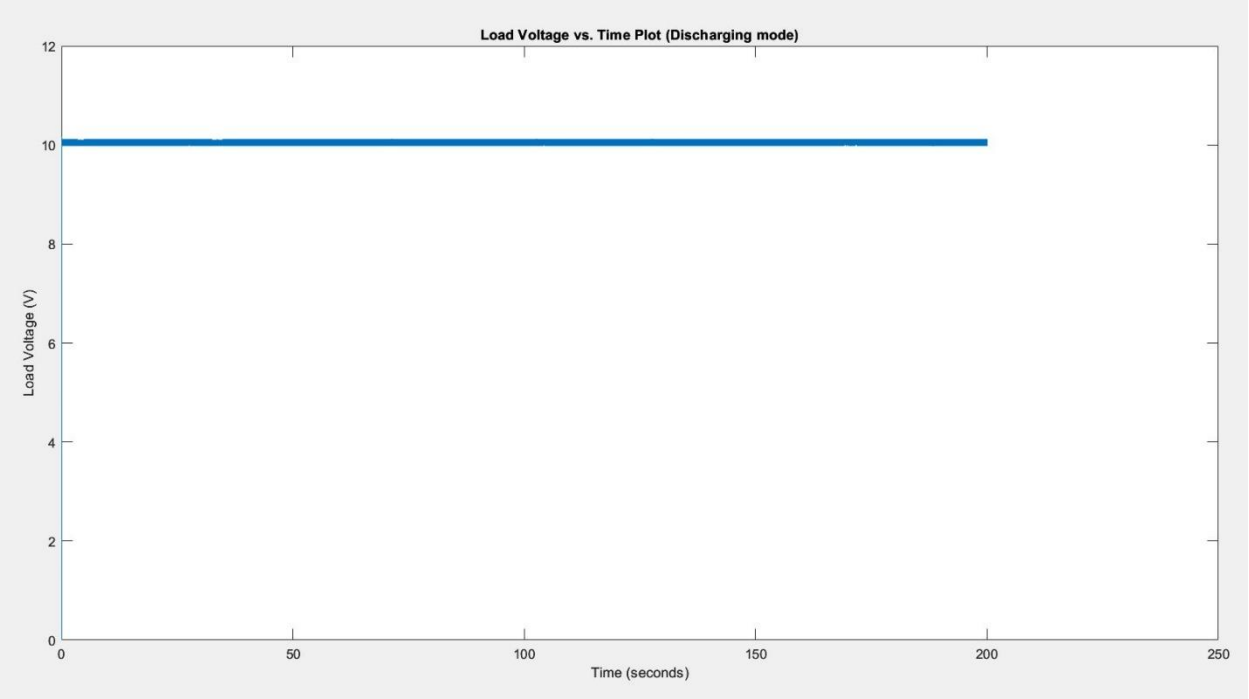


*Figure 7-20 Load Voltage vs. Time Plot*

From the four plots above, it is clear that the battery is being discharged from 91% to 90% SOC and it will keep behaving the same as long as it's not connected to the charger or the gird. The discharging current behaves constantly at around +5 A where the positive sign indicates that the battery is being discharged. The battery voltage starts decreasing while the battery is being discharged, but the load voltage is controlled at 10 V which ensures that the EV load will always receive a constant required voltage at a constant discharging current.

# 8 Conclusion

To conclude, the battery management system (BMS) is a critical part of electric vehicles (EVs) and is responsible for monitoring and controlling the performance of the battery pack, particularly in the areas of battery modelling, state estimation, and battery charging. The accurate modelling and estimation of battery internal states and parameters are crucial in providing a comprehensive understanding of the battery's operating status in EV applications. The primary functions of the BMS are to ensure the safety of the battery pack, optimize its performance, and extend its lifespan.

Effective battery management has a significant impact on the overall performance and efficiency of an EV, including factors such as range, acceleration, and charging time. As such, BMS technology is continually evolving to meet the growing demands of the EV market. Additionally, the development of BMS technology has significant implications for the future of transportation and the environment. As more vehicles transition to electric power, the need for reliable and efficient battery management will only continue to increase.

In summary, the battery management system is a crucial component of electric vehicles that plays a critical role in ensuring the safety, performance, and longevity of the battery pack. Ongoing advancements in BMS technology will drive the widespread adoption of electric vehicles and contribute to reducing the environmental impact of transportation.

# 9 Appendices

## 9.1 Codes

Model initialization code

```
% SOC Lookup Table breakpoints
SOC_LUT = (0:0.1:1)';

%% Known Values

% Battery capacity
% Measured by coulomb counting the discharge curve
Capacity = 27.6250; %Ampere*hours

% Charge deficit at start of data set

%% Estimated Parameters - Initial starting points before estimation

% Em open-circuit voltage vs SOC
Em = 3.8*ones(size(SOC_LUT)); %Volts

% R0 resistance vs SOC
R0 = 0.01*ones(size(SOC_LUT)); %Ohms

% R1 Resistance vs SOC
R1 = 0.005*ones(size(SOC_LUT)); %Ohms

% C1 Capacitance vs SOC
C1 = 10000*ones(size(SOC_LUT)); %Farads

%% Load Dataset
load('LiBatt_PulseData.mat')
```

- SOH calculations

```
function [soh,av_cap]  = SOH_Calc(num_cycles)

%   this code will mainly count the number of cycles of charging-discharging
and calculte the new total capacity of the
%   batteries per the following paper
%   (https://doi.org/10.1063/1.5012602). the calculations is mainly based
%   on an experimental results and curve fitting for the relation between the
normalized capacity and the number of cycles
%   main script of the project as it needs to run only once at the begaining.

if(num_cycles>10)
```

```
    normaliz_capacity=((-3.72420611065173e-15)*(num_cycles^6)+
       (3.75024849118566e-12) *(num_cycles^5) -(1.44810117823229e-
9)*(num_cycles^4)+ (2.64463491236913e-07)*(num_cycles^3)  -
(2.23630419461362e-5) *(num_cycles^2)+
       (0.000381471576336523)*(num_cycles)+0.984192557022104)*27.6250;
    soh=((-3.72420611065173e-15)*(num_cycles^6)+    (3.75024849118566e-12)
*(num_cycles^5)    -(1.44810117823229e-9)*(num_cycles^4)+ (2.64463491236913e-
07)*(num_cycles^3)  -(2.23630419461362e-5) *(num_cycles^2)+
       (0.000381471576336523)*(num_cycles)+0.984192557022104);
    av_cap=  normaliz_capacity;
else
    soh=1;
    av_cap=27.6250;
end
```

## 9.2 Simulink models

### 9.2.1 SOC models

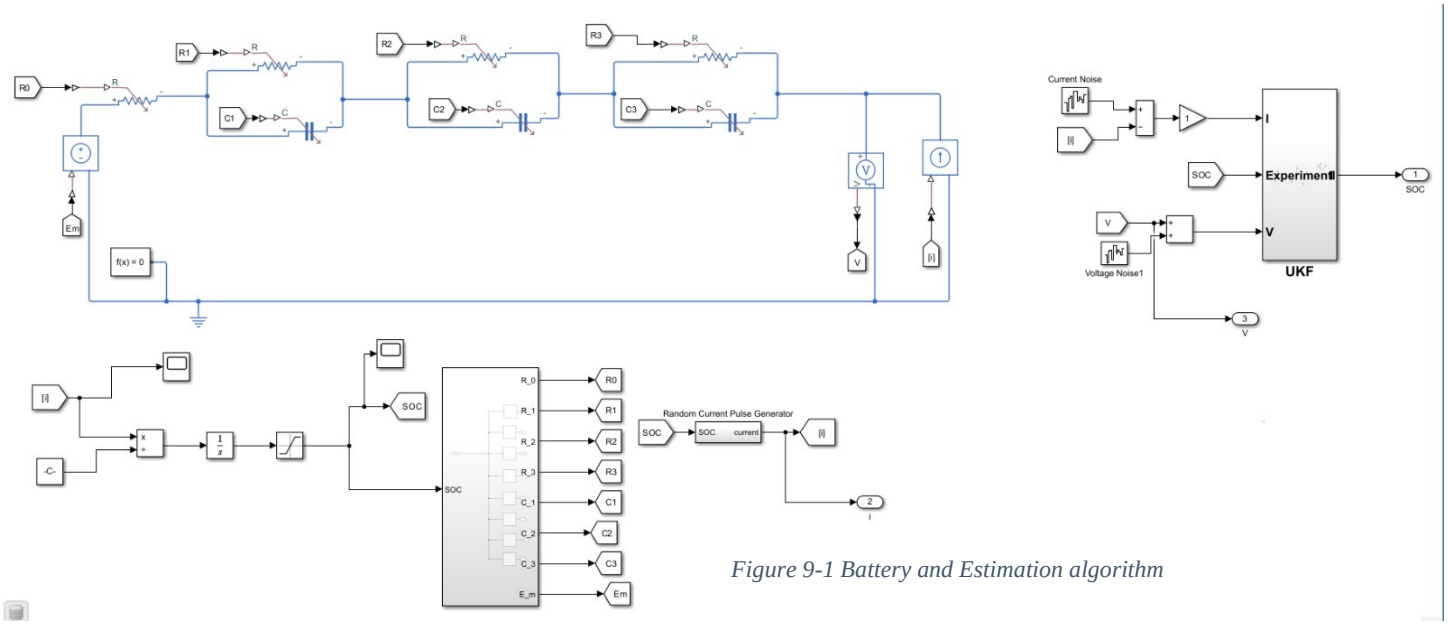


*Figure 9-1 Battery and Estimation algorithm*

## 9.2.2 SOH models

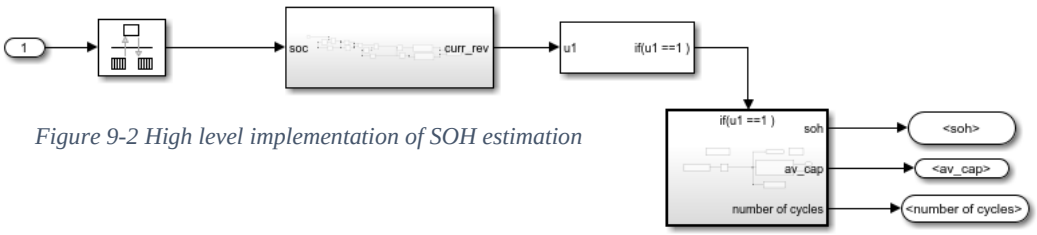


*Figure 9-2 High level implementation of SOH estimation*

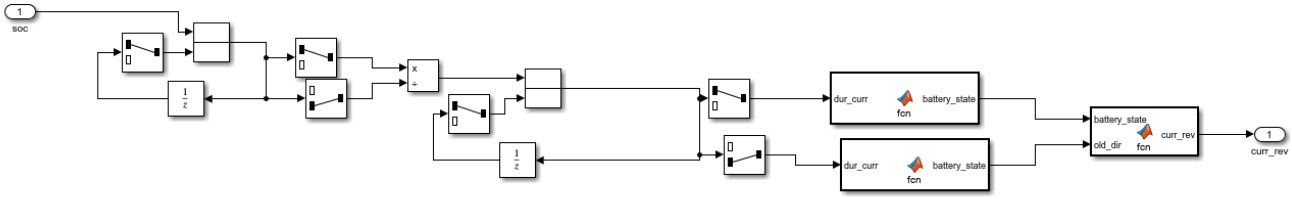


*Figure 9-3 mid-level implementation of SOH algorithm*

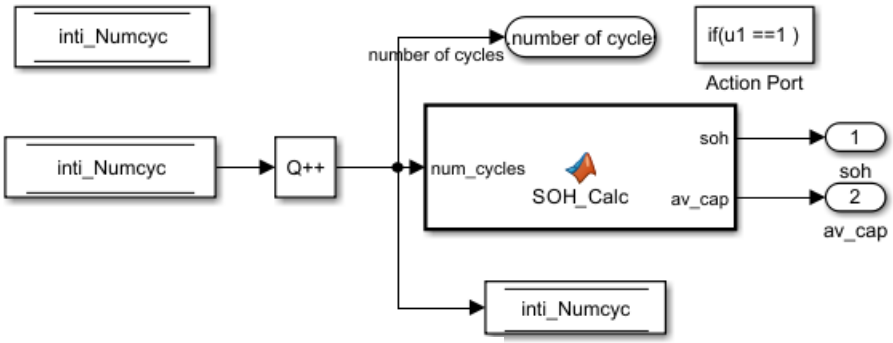


*Figure 9-4 Low-level implementation of SOH algorithm*

## 9.2.3 Charging and Discharging Control models

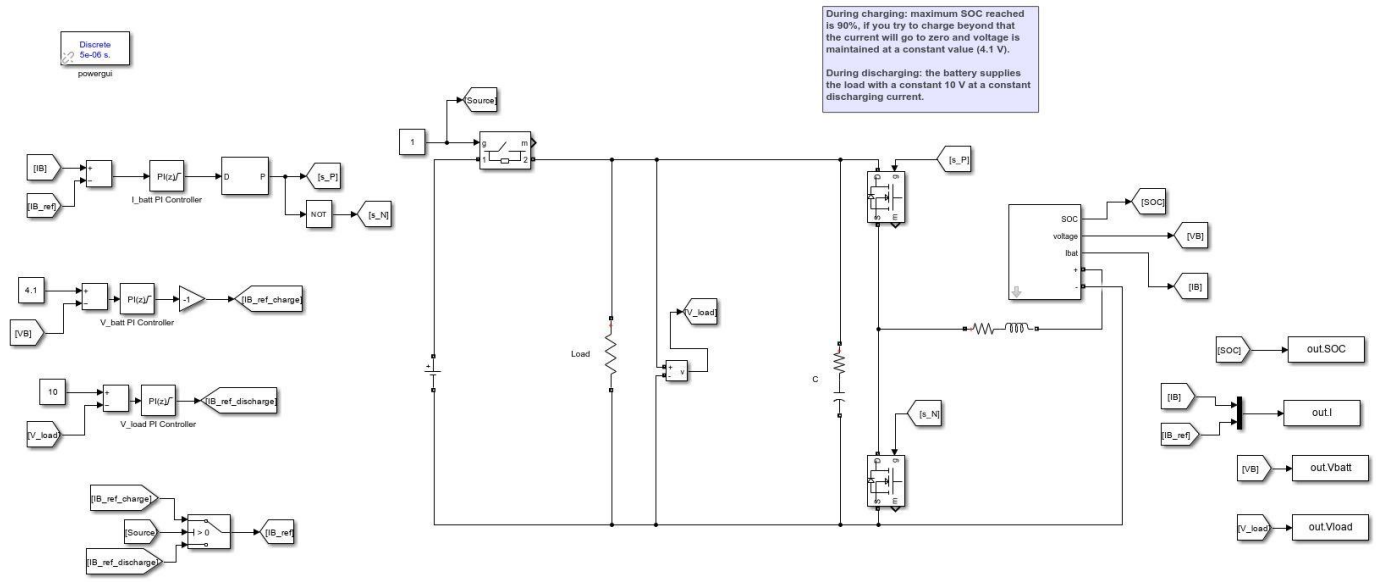


*Figure 9-5 Battery Charging Model*

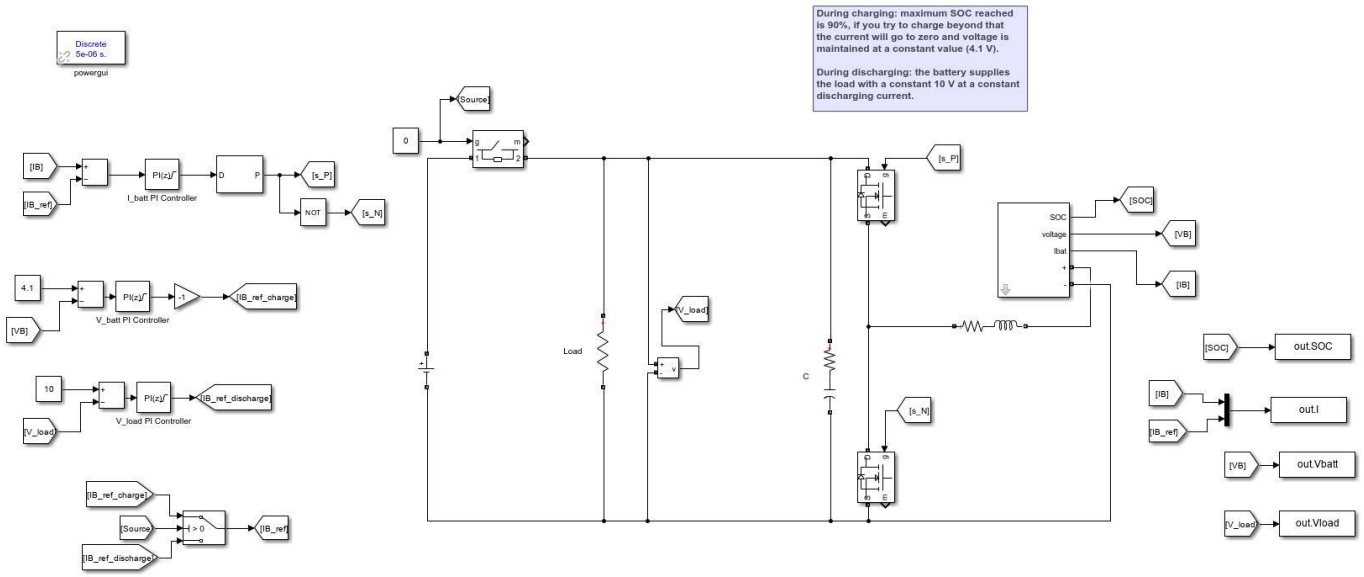


*Figure 9-6Battery Discharging Model*

## 9.2.4 Cell Balancing models

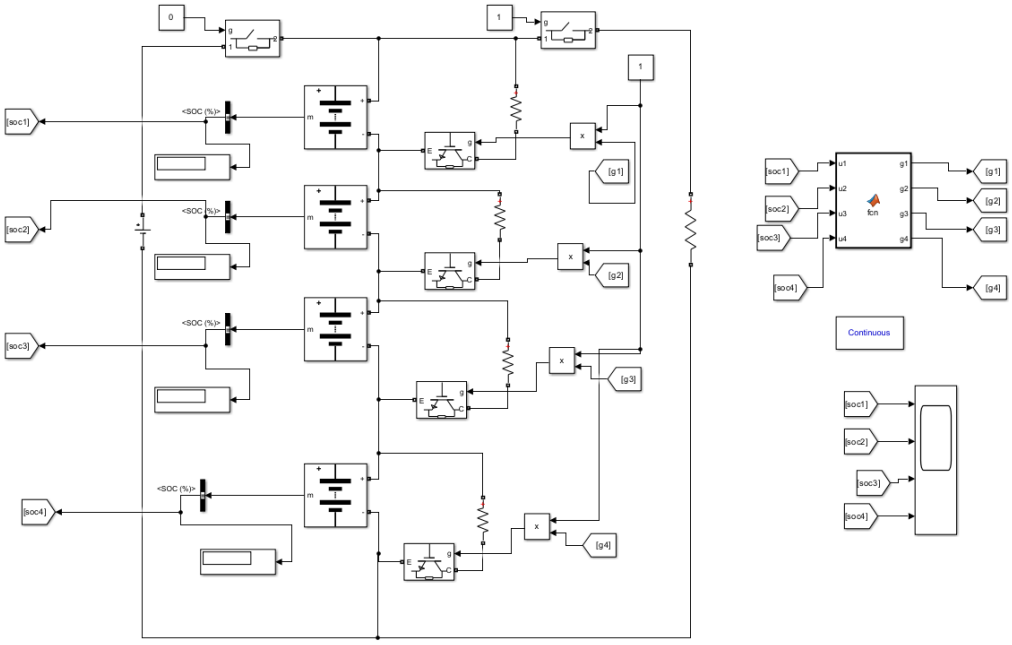


*Figure 9-7passive Balancing model*

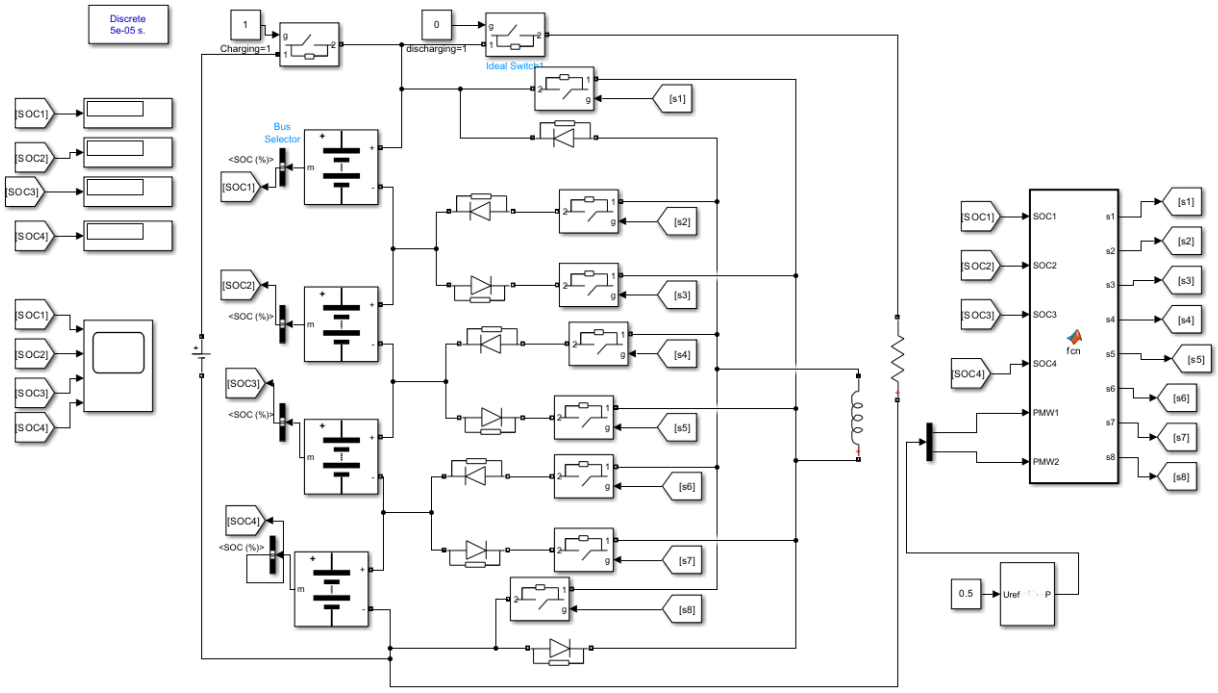


*Figure 9-8Inductor based Active Balancing model*

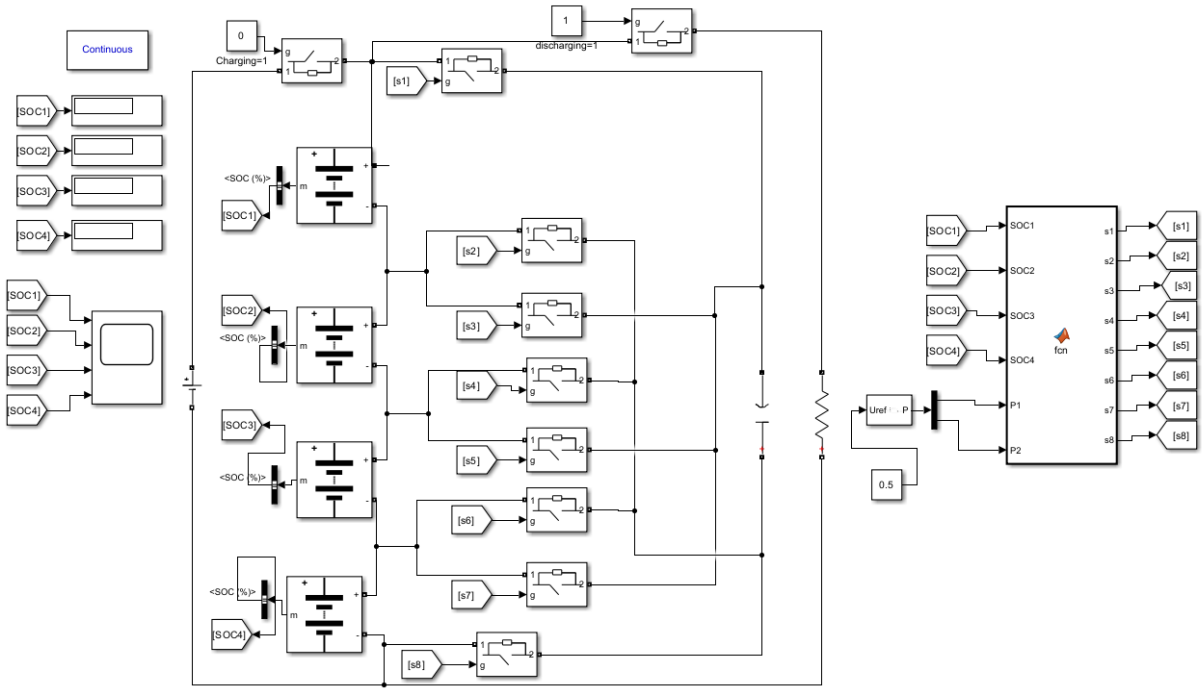


*Figure 9-9Capacitor based Active Balancing mode*

# 10 References


1. Nejad, S.; Gladwin, D.T.; Stone, D.A. A systematic review of lumped-parameter equivalent circuit models for real-time estimation of lithium-ion battery states. J. Power Sour. 2016, 316, 183–196. [CrossRef]

2. Deng, H.; Yang, L.; Deng, Z.W. Parameter identification and SOC estimation of lithium-ion battery based on electrochemical mechanism model. J. Univ. Shanghai Sci. Technol. 2018, 40, 557–565.

3. Wang, G.F.; Wang, S.L.; Yu, C.M. Improved battery equivalent circuit modeling combined with Thevenin and PNGV models. Autom. Instrum. 2021, 42, 45–49.

4. Wang, W.Q.; Sun, Y.Q.; He, Y. Variable parameter PNGV model for lithium iron phosphate lithium-ion battery. Battery 2020, 50, 40–44.

5. Wei, Z.H.; Song, S.X.; Xia, H.Y. Estimation of State of Charge of Li-ion Battery Based on Random Forest. J. Guangxi Normal Univ. 2018, 36, 27–33.

6. Hu, J.; Gao, Z.W. Data-driven SOC prediction of electric vehicle power battery. Autom. Eng. 2021, 43, 1–9.

7. Yang, D.; Wang, Y.; Pan, R.; Chen, R.; Chen, Z. State-of-health estimation for the lithium-ion battery based on support vector regression. Appl. Energy 2017, 227, 273–283. [CrossRef]

8. Battery University. (2022, March 3). *BU-808: How to prolong lithium-based batteries*. Battery University. Retrieved March 24, 2023, from https://batteryuniversity.com/article/bu-808-how-to-prolong-lithium-based-batteries.

9. Xu, B., Oudalov, A., Ulbig, A., Andersson, G., & Kirschen, D. S. (2018). Modeling of lithium-ion battery degradation for Cell Life Assessment. *IEEE Transactions on Smart Grid*, *9*(2), 1131–1140. https://doi.org/10.1109/tsg.2016.2578950

10. Andrea(2023). ImageDigitizer (https://www.mathworks.com/matlabcentral/fileexchange/49009-image-digitizer), MATLAB Central File Exchange. Retrieved February 23, 2023.
11. Z. Chen, L. Yang, X. Zhao, Y. Wang, and Z. He, "Online state of charge estimation of Li-ion battery based on an improved unscented Kalman filter approach," *Appl. Math. Model.*, vol. 70, pp. 532–544, 2019, doi: 10.1016/j.apm.2019.01.031.
12. R. Ahmed *et al.*, "Model-Based Parameter Identification of Healthy and Aged Li-ion Batteries for Electric Vehicle Applications," *SAE Int. J. Altern. Powertrains*, vol. 4, no. 2, pp. 233–247, 2015, doi: 10.4271/2015-01-0252.
13. C. Taborelli and S. Onori, "State of charge estimation using extended Kalman filters for battery management system," *2014 IEEE Int. Electr. Veh. Conf. IEVC 2014*, 2014, doi: 10.1109/IEVC.2014.7056126.
14. T. Huria, M. Ceraolo, J. Gazzarri, and R. Jackey, "High fidelity electrical model with thermal dependence for characterization and simulation of high power lithium battery cells," *2012 IEEE Int. Electr. Veh. Conf. IEVC 2012*, no. April 2015, 2012, doi: 10.1109/IEVC.2012.6183271.
15. Y. Tian, B. Xia, W. Sun, Z. Xu, and W. Zheng, "A modified model based state of charge estimation of power lithium-ion batteries using unscented Kalman filter," *J. Power Sources*, vol. 270, pp. 619–626, 2014, doi: 10.1016/j.jpowsour.2014.07.143.
16. J. Zhang, Y. Wei, and H. Qi, "State of charge estimation of LiFePO4 batteries based on online parameter identification," *Appl. Math. Model.*, vol. 40, no. 11–12, pp. 6040–6050, 2016, doi: 10.1016/j.apm.2016.01.047.
17. W. He, N. Williard, C. Chen, and M. Pecht, "State of charge estimation for electric vehicle batteries using unscented kalman filtering," *Microelectron. Reliab.*, vol. 53, no. 6, pp. 840–847, 2013, doi: 10.1016/j.microrel.2012.11.010.
18. Moore, S.W. and Schneider, P.J. (2001) "A review of cell equalization methods for lithium ion and Lithium Polymer Battery Systems," *SAE Technical Paper Series* [Preprint]. Available at: https://doi.org/10.4271/2001-01-0959.

19. Piao, C. *et al.* (2015) “Lithium-ion battery cell-balancing algorithm for battery management system based on real-time outlier detection,” *Mathematical Problems in Engineering*, 2015, pp. 1–12. Available at: https://doi.org/10.1155/2015/168529.
20. Lee, Y., Jeon, S. and Bae, S. (2016) “Comparison on cell balancing methods for energy storage applications,” *Indian Journal of Science and Technology*, 9(17). Available at: https://doi.org/10.17485/ijst/2016/v9i17/92316.
21. Dennis Corrigan, et al., "Ovonic Nickel-Metal Hydride Electric Vehicle Batteries", the 12th International Electric Vehicle Symposium (EVS-12), Anaheim, CA, Dec., 1994

22. Z. Zhang, L. Zhang, L. Hu, and C. Huang, “Active cell balancing of lithium-ion battery pack based on average state of charge,” *International Journal of Energy Research*, vol. 44, no. 4, pp. 2535–2548, 2020. doi:10.1002/er.4876

23. M.-K. Tran *et al.*, “Concept review of a cloud-based Smart Battery Management System for lithium-ion batteries: Feasibility, logistics, and functionality,” *Batteries*, vol. 8, no. 2, p. 19, 2022. doi:10.3390/batteries8020019

24. N. Samaddar, N. Senthil Kumar, and R. Jayapragash, “Passive cell balancing of Li-ion batteries used for automotive applications,” *Journal of Physics: Conference Series*, vol. 1716, no. 1, p. 012005, 2020. doi:10.1088/1742-6596/1716/1/012005

T. Duraisamy and K. Deepa, “Evaluation and comparative study of cell balancing methods for lithium-ion batteries used in electric vehicles,” *International Journal of Renewable Energy Development*, vol. 10, no. 3, pp. 471–479, 2021. doi:10.14710/ijred.0.34484